How Exposed are Banks to Physical Climate Risk?

Kristle R. Cortés* Konark Saxena† Mandeep Singh‡

February 6, 2026

Abstract

This paper develops a factor-based framework to measure US banks' exposure to physical climate risk. Using monthly temperature data, we estimate that the US banking sector's systemic physical climate risk is approximately 500 billion dollars, equivalent to roughly one-quarter of the sector's reported equity, by the late 2010s. Exposed banks also reduce lending to small businesses, especially in counties without branches. The framework offers a scalable, disclosure-free measure of physical climate risk, illustrating how climate vulnerabilities are transmitted into credit markets and have direct implications for supervision and stress testing.

JEL Classification Codes: G21, Q54
Keywords: Temperature anomaly factors, Physical climate risk, Credit availability.

*UNSW Business School, UNSW Sydney, Australia. Email: kristle.cortes@unsw.edu.au.
†ESCP Business School, Paris, France. Email: ksaxena@escp.eu.
‡Discipline of Finance, University of Sydney, Australia. Email: mandeep.singh@sydney.edu.au.
We thank Phil Strahan, Steven Ongena, Frank Weikai Li, Emirhan Ilhan, participants at the Asia-Pacific Corporate Finance Online Workshop (2025), the New Zealand Finance Meeting (2025), and seminar participants at the University of Sydney, the Reserve Bank of Australia, and the UNSW Institute for Climate Risk and Response for valuable feedback. All errors are our own.

1 Introduction

The increasing severity of natural disasters creates financial vulnerabilities by impairing asset values and loan performance. Yet disasters, as episodic events that can occur even in an unchanging climate, may not capture the gradual and long-term changes in climate that underlie physical climate risk. As these changes accumulate across borrowers and markets, they can reshape banks' exposures to credit and collateral risk, raising an important question: to what extent are banks exposed to physical climate risk? This question is now central to policy debates among central banks (BoE, 2021, 2022, 2023; ECB, 2020, 2022a,b)) and international institutions (BCBS, 2021, 2022b,a; TCFD, 2017) because banks are key intermediaries in the economy and their exposure determines how physical climate risk contributes to financial instability.

To address this question, this paper develops a framework to quantify the physical climate risk borne by the US banks and the banking sector. We construct systematic temperature anomaly factors that quantify physical climate risk across US counties (Roll & Ross, 1980; Connor & Korajczyk, 1988). These factors, along with the counties' exposure to them, are linked to the probability and severity of natural disasters, providing an economically relevant measure of physical climate stress to capture underlying climate dynamics. We examine whether these physical climate risk factors are reflected in financial market outcomes and banks' intermediation behavior. We estimate bank-level climate betas that measure each institution's sensitivity to systematic temperature anomaly factors. These exposures vary substantially across banks and over time and are associated with heightened stock return volatility, particularly among smaller and more geographically concentrated banks. Banks with greater exposure to the dominant temperature anomaly factor reduce credit supply to small businesses, indicating that physical climate risk affects real economic activity through the lending channel. Aggregating these exposures following Jung et al. (2025), we estimate that systemic physical climate risk in the US banking sector reached approximately 500 billion dollars in the late 2010s. The proposed framework is scalable, data-driven, and suitable for integration into risk management, stress testing, and supervisory oversight.

The literature has advanced in measuring climate transition risks, often using portfolio-based factors constructed from firms' carbon intensity, environmental ratings, or exposure to stranded assets, proxied by industry classification (Bolton & Kacperczyk, 2021; Pástor et al., 2021; Jung et al., 2025). These approaches arguably capture the financial risks associated with an economy transitioning to a greener self. Jung, Engle, et al. (2024) link real estate investment trust (REIT) returns to property damages, offering an asset-based view of physical climate risk. Economic outcomes also reflect the offsetting effects of local adaptation strategies (Hsiang, 2016), which confounds the effects of physical climate risk. As temperature is governed by physical processes rather than policy responses, systematic movements in temperature reflect the dynamics of the climate system itself. Estimating factors from gridded temperature anomalies, therefore, uncovers the dominant co-movements driven by shared physical forces, rather than by local adaptation or transition behaviors that shape policy responses but not the underlying temperature dynamics. The resulting temperature anomaly factors thus capture the exogenous common component of climate variability.

The first four temperature anomaly factors explain 89 percent of the variation in observed temperature anomalies across 3,108 US counties, with the leading factor alone accounting for approximately 60 percent of that variation. We validate the temperature anomaly factors by showing that the temperature anomalies they predict are associated with the frequency and severity of impending natural disasters at the county level. Time-series regression tests indicate that these factors contain information not already captured by traditional asset pricing factors, and incorporating them into standard models improves explanatory power. While the temperature anomaly factors do not command a risk premium in average returns, they are associated with higher return volatility for bank and financial stocks, consistent with their role as long-horizon, non-diversifiable physical shocks that primarily operate through heightened uncertainty and downside risk rather than expected returns. Building on these validation exercises, we estimate bank-level climate betas that quantify the sensitivity of banks' stock returns to systematic temperature anomaly factors. These betas serve as the foundation for

quantifying bank-specific physical climate risk and, in aggregate, for estimating systemic physical climate risk for the US banking sector.

Our estimates indicate that systemic physical climate risk for publicly traded US banks reached approximately 500 billion dollars at its peak, with three notable surges in 2005, 2012, and 2018–2019. These peaks correspond to periods of heightened climate stress and are driven by distinct systematic temperature anomaly factors. As they are not observed during the sample period considered in the study, non-linear climate tipping points are not incorporated in our framework. We show that the variance explained by the first four factors, individually and in aggregate, remains stable over time. This stability supports interpreting our estimates as measures of systematic exposure rather than artifacts of a particular sample window. Our framework accommodates future changes in climate dynamics as new data arrive. Consequently, our framework provides a lower bound of systemic physical climate risk.

Next, we examine whether banks' exposure to temperature anomalies affects their lending. Lending is a key channel through which banks transmit shocks to the real economy, and small businesses provide an especially informative setting because they are highly reliant on banks, locally concentrated, and lack access to external financing or hedging. We focus on the first temperature anomaly factor, which accounts for approximately 60 percent of the variation across US counties and is nearly perfectly correlated with the cross-sectional average temperature anomaly. We use a combination of high-dimensional fixed effects to control for credit demand and endogenous matching between small businesses in a county and a bank. Our results indicate that a standard deviation increase in exposure is associated with 2 fewer small business loan originations and a reduction of approximately 32 thousand in total lending volume. This decline is sizable, equivalent to approximately 18 percent and 9 percent of the average total number and volume of small-business loan originations, respectively.

A physical branch presence enables banks to gather information, build relationships, and preserve rents, thereby reducing the likelihood that they will withdraw credit in response to rising physical climate risk. Consistent with this idea, we find that the

decline in lending associated with exposure to the first temperature anomaly factor is concentrated in markets outside a bank's branch network. This result highlights the role of branch networks in buffering small businesses from credit contractions driven by physical climate risk, as banks maintain lending commitments in regions where they have established physical presence.

The geographic interpretation of these factors is straightforward. Each statistical factor captures systematic temperature variation concentrated in particular regions of the US. The factor loadings map cleanly onto geography as counties with similar latitudes, longitudes, and climatic regimes share similar exposures. In this sense, the factors are not abstract statistical objects but rather realizations of temperature patterns localized to a geography. For instance, the first factor reflects the average warming trend, whereas subsequent factors distinguish regional contrasts such as coastal versus continental or northern versus southern variability. Because these geographic modes of temperature variation drive the probability and severity of climate hazards, the estimated factors are physical climate-risk measures. They summarize the strength with which each region's temperature anomalies covary over time with dominant large-scale climate patterns, such as nationwide warming or regional contrasts driven by oceanic and atmospheric circulation. Because banks operate across geographies, their portfolios inherit these co-movements: a bank exposed to counties that move with a given temperature pattern is correspondingly exposed to that underlying physical climate process.

We test whether the statistical factors align with the geographical interpretation. We construct location-based temperature anomaly factors by pre-specifying counties' loadings as a function of latitude and longitude relative to a reference county. The results confirm that systematic variation in temperature anomalies closely coincides with the geography, as the correlation between the two sets of factors is high, and that the resulting estimates of systemic physical climate risk are economically consistent with those based on factor analysis. We view the location-based factors as a validation exercise rather than a substitute. The factor-analysis approach is data-driven; hence, it

is a more parsimonious way to extract systematic variation across US regions. Nonetheless, both approaches capture economically meaningful dimensions of vulnerability to climate hazards and adaptive capacity shaped by geography, and the close alignment of their results provides reassurance about the robustness of our framework.

Our framework is amenable to global temperature data. Studying global temperature anomaly data is fruitful for at least two reasons. First, large-scale atmospheric and oceanic processes may influence local weather. Second, many of the listed US banks are large and operate in multiple countries. The global temperature anomaly factors are not simple proxies for their US counterparts, as correlations across the two factor sets are relatively low. Using the global temperature anomaly factors, we estimate systemic climate risk at approximately 470 billion dollars, with exposures clustering during periods of broader financial stress.

To our knowledge, this is the first study to document a temperature-anomaly factor structure and connect it to financial risk. The factors summarize how temperature co-moves across regions and how these co-movements imply non-diversifiable exposures to physical climate risk, creating sector-wide vulnerabilities for banks. This framework provides a new empirical basis for measuring physical climate risk in the financial system.

This study contributes to the climate finance literature by extending approaches that quantify systemic risk into the domain of physical climate risk. A growing set of papers aims to measure financial stress arising from climate exposures. These studies build on the SRISK and capital shortfall framework (V. Acharya et al., 2012; V. V. Acharya et al., 2013; V. Acharya et al., 2014; Brownlees & Engle, 2017), which link firm-level vulnerabilities to sector-wide fragility. Within climate finance, Jung et al. (2025) propose CRISK to measure capital shortfalls under transition stress scenarios. Jourde & Moreau (2024) identify transition risk as the main driver of financial instability in European institutions. Building on the observation that climate-induced disasters adversely affect real estate values, Jung, Engle, et al. (2024) use real estate investment trust (REIT) returns to construct a market-based proxy for banks' physical climate risk exposure.

Regulators and researchers have turned to stress-testing and network-based approaches to assess broader financial vulnerabilities (V. Acharya et al., 2014; Battiston et al., 2017; Roncoroni et al., 2021). This paper extends this literature by developing a framework that uses physical climate data to extract systematic risk factors, which we then link to financial market outcomes to measure banks' and the banking sector's exposures. Our approach is related to earlier work using bank stock price sensitivities to infer latent bank characteristics, such as diversification (Baele et al., 2007), the effect of mergers (Vander Vennet, 1996), and efficiency (Vennet, 2002), but extends this logic to the measurement of systematic physical climate risk using endogenously constructed temperature anomaly factors.

Our analysis also complements prior studies that examine climate transition and physical risk. A growing body of literature examines how climate policies, technological shifts, and carbon repricing affect financial institutions (Kacperczyk & Peydró, 2022; B. Bruno & Lombini, 2023; Giannetti et al., 2023; Haushalter et al., 2023; Green & Vallee, 2024; Jung, Santos, & Seltzer, 2024; Beyene et al., 2024; Carattini et al., 2025; Cicco et al., 2025; Benincasa et al., 2025; Duan et al., 2025). While banks have adjusted their lending practices in response to transition risks (Delis et al., 2019; Degryse et al., 2023; Altavilla et al., 2024; Ivanov et al., 2024; Kim et al., 2025; Blickle et al., 2025), empirical evidence shows inconsistent divestment from high-emission sectors and limited impact of net-zero commitments on financed emissions (Sastry, Verner, & Marques Ibanez, 2024; Morse & Sastry, 2025). Some studies focus on the economic implications of physical climate risk by using natural disasters (Klomp, 2014; Cortés & Strahan, 2017; Koetter et al., 2020; Kousky et al., 2020; Blickle et al., 2021; Correa et al., 2022; Nguyen et al., 2022; Sastry, 2022; Sastry, Sen, & Tenekedjieva, 2024; Rajan & Ramcharan, 2023; Abedifar et al., 2024; Kruttli et al., 2024) as a source of exogenous variation. V. V. Acharya et al. (2022) show extreme heat stress exposure is priced in the US municipal and corporate bond and equity markets. Li et al. (2025) study how extreme rainfall is priced in Chinese municipal corporate bond markets and show that urban climate adaptation mitigates the increase in borrowing cost, highlighting the fiscal value of investment in climate

resilience. We complement this literature by proposing a forward-looking measure of physical climate risk. We extract systematic factors from temperature anomalies, a key driver of both disaster intensities and adaptation.

2 Data description

2.1 Temperature data

We source monthly mean temperature data from the Climatic Research Unit (CRU) at the University of East Anglia. The dataset has a $0.5° \times 0.5°$latitude-longitude resolution. These dimensions are equivalent to approximately 55 kilometers at the equator. We match counties to the nearest grid using centroid-based distance matching. This approach ensures unique time-consistent matching as the locations of counties and grids do not vary over time. The sample spans 1951–2019. Following the NASA Goddard Institute for Space Studies (GISS) methodology, we use the 1951–1980 period as the reference for estimating county-month temperature anomalies.

2.2 Banks' financial and lending data

We source stock return data from the Center for Research in Security Prices (CRSP) via Wharton Research Data Services (WRDS), the standard source for US equity prices, returns, and market indices. To link stock-level information with bank financials and lending activity, we rely on the CRSP–FRB link dataset provided by the Federal Reserve Bank of New York. Factor returns and 48 industry portfolios are obtained from Kenneth French's data library.

We compile bank balance sheet information from quarterly Call Reports and measure deposit funding and branch networks using the Summary of Deposits dataset. Deposits are aggregated at the bank–county–year level, and branch counts are recorded by county. To capture banks' lending to small businesses, we utilize data collected under the Community Reinvestment Act (CRA), which requires depository institutions to report on their efforts to meet local credit needs while maintaining sound and safe practices. Our analysis focuses on the CRA originations dataset, which records the

number and volume of loans made to small agricultural farms at the bank–county–year level from 1997 to 2017. We align the CRA data with Call Report information using year-end balance sheet values.

2.3 Disaster damages data

We use county-level natural disaster data from the Spatial Hazard Events and Losses Database for the United States (SHELDUS). The database records major weather events, including thunderstorms, hurricanes, floods, wildfires, and tornadoes, along with event dates, affected locations, and direct damages (property and crop losses, injuries, and fatalities) beginning in 1960. Our analysis focuses on weather-related hazards, including coastal storms, droughts, floods, hail, heatwaves, hurricanes, landslides, lightning, severe storms, tornadoes, wildfires, wind events, winter weather, fog, and avalanches. Geological hazards, such as earthquakes, volcanoes, tsunamis, and seiches, are excluded because they are unrelated to temperature anomalies. We construct a county–month panel spanning 1984–2019 by aggregating individual hazard records at the county–hazard–month level. All damage variables are adjusted to 2022 dollars and scaled by county population to provide comparable, per-capita measures of disaster intensity. This structure yields a consistent panel of disaster occurrence and severity over time.

3 Methods and results

3.1 Estimating temperature anomaly factors

3.1.1 Factor analysis of temperature anomalies across US counties

Increases in anomalous temperature amplify the frequency and intensity of climate disasters (IPCC, 2001, 2012). Local climate adaptation, more likely in more exposed regions, can also offset observable economic losses from disasters. Because temperature anomalies capture the physical processes that generate both disasters and subsequent adaptation responses, they provide a fundamental measure of climatic variation that is exogenous to economic activity. We, therefore, focus on temperature anomalies to isolate

the underlying physical signal of climate change rather than its economic consequences. Co-movements in regional temperature anomalies reveal shared exposure to large-scale climate dynamics, which we interpret as a systematic component of physical climate risk.

To model the temperature anomalies as a factor model, we define the anomaly for county c in month m and year y as:

$$\Delta \mathbb{T}_{cmy} = \mathbb{T}_{cmy} - \bar{\mathbb{T}}_{cm} \qquad y \geq 1984 \tag{1}$$

where $\mathbb{T}_{cmy}$ is the observed temperature, and $\bar{\mathbb{T}}_{cm}$ is the historical average temperature for county c in month m, computed over 1951–1980 reference period: $\frac{1}{30}\sum_{y=1951}^{1980} \mathbb{T}_{cmy}$. This approach captures deviations from historical norms and accounts for geographic and seasonal variation by anchoring each county's anomaly to its long-term monthly average.

Figure 1 summarizes temperature and temperature anomaly data. Figure 1a displays the spatial distribution of average temperature and temperature anomalies over the 36-year period beginning in January 1984. The map of average temperatures shows a clear geographic gradient, with warmer regions concentrated at lower latitudes and cooler regions at higher latitudes. The spatial distribution of temperature anomalies does not exhibit a monotonic pattern.

[Insert Figures 1 Here]

The left panel of Figure 1b plots the distribution of average temperatures over 1951–1980, 1984–2000, and 2001–2019. The distribution shifts to the right across periods, reflecting both higher mean temperatures and a greater incidence of extreme heat. The right panel displays the distribution of temperature anomalies for the periods 1984–2000 and 2001–2019. The mean anomaly rises from 0.3 degrees Celsius in the earlier period (range: –0.2 to 1 degrees Celsius) to 0.8 degrees Celsius in the later period (range: 0.4 to

1.4 degrees Celsius), a 2.6-fold increase. These changes suggest that some regions are already approaching the 1.5 degrees Celsius threshold outlined in the Paris Agreement and that abnormally high temperatures have become increasingly common.

We model temperature anomaly, $\Delta\mathbb{T}_{ct}$, as a linear factor model, with a set of latent factors driving variation in temperature anomalies across counties. Formally, we write:

$$\Delta\mathbb{T}_{ct} = \sum_{k=1}^{K} \lambda_{ck} f_{kt} + \epsilon_{ct}, \tag{2}$$

where f_{kt} represents the k^{th} latent factor's realization at time t, capturing systematic components of temperature anomalies that are common across counties. λ_{ck} denotes the factor loading for county c on the k^{th} factor, indicating the sensitivity of temperature anomalies in county c to factor k. ϵ_{ct} is the idiosyncratic error term. The latent factors summarize systematic variation in temperature anomalies across US counties.

Our temperature anomaly data cover 3,108 contiguous counties over 432 months, from January 1984 to December 2019. We use factor analysis to decompose temperature anomalies into systematic and idiosyncratic components (Connor & Korajczyk, 1988). We retain the first K factors based on the cumulative variance explained.

[Insert Table 1 Here]

[Insert Figure 2 Here]

Table 1 and Figure 2 report summary statistics, and time series plots, respectively, of the first four latent factors ($\{f_{kt}\}_{k=1}^{4}$) extracted from standardized county-level temperature anomalies using factor analysis. Panel A of Table 1 shows that these four factors jointly account for 88.9 percent of the total variation. The first factor alone explains 59.8 percent of the variation. Together, these factors capture the dominant sources of temperature fluctuations across US counties. In Panel B, we report county-level factor loadings. A majority of counties load positively on the first factor. In contrast, loadings for other temperature anomaly factors exhibit heterogeneity among counties.

[Insert Figure 3 Here]

In Figure 3, we show the spatial distribution of county loadings (λ_{ck}). Counties in the eastern and southeastern United States, the northern Midwest and Northeast, the arid Southwest, and the West and East coasts of the US exhibit higher loadings for the first, second, third, and fourth factors, respectively. These regional patterns align with the influence of subtropical and maritime air masses and El Niño–Southern Oscillation (ENSO) related variability documented in studies (Wallace & Hobbs, 2006; Trenberth et al., 2007; IPCC, 2012). These patterns highlight the role of geography in determining long- and short-term regional climate driven by a small number of common factors.

In Figure C.1, we assess the stability of the temperature-anomaly factor structure over time. For each terminal year from 2001 to 2019, we re-estimate the factors using an expanding monthly sample that begins in January 1984 and plot the proportion of total cross-location variation explained by the first four factors. The proportion of variance explained by each factor is relatively stable across estimation windows, indicating that the covariation of temperature anomalies across U.S. counties remains largely unchanged as additional climate realizations are incorporated over the sample period considered in this study. This exercise, however, does not test for nonlinear climate tipping points arising from threshold effects. Rather, it establishes that the factor space used to quantify systematic physical climate exposure is stable, supporting the interpretation of our estimates as measures of exposure that can be updated as new information becomes available.

3.1.2 Validating temperature anomaly factors

Disaster occurrences alone do not establish climate change, since extreme events can also occur in stable climates. Temperature anomalies provide a continuous and direct signal of climate trends. To validate the anomaly factors, we test whether factor realizations and counties' loadings on them, the systematic component of temperature variability, predict local disaster outcomes. We also include the residualized temperature

anomaly ($\Delta\mathbb{T}_{ct} - \sum_{k=1}^{4} \hat{\lambda}_{ck}\hat{f}_{kt}$) as a control for unsystematic local shocks orthogonal to the common temperature anomaly factors.

[Insert Table 2 Here]

Table 2 reports the association between temperature anomaly factors and subsequent disaster outcomes. In Panel A, we use the fitted value of temperature anomaly ($\sum_{k=1}^{4} \hat{\lambda}_{ck}\hat{f}_{kt}$) of each county's temperature anomaly and the residual anomaly as regressors. The coefficient on the predicted temperature anomaly is positive and significant across all measures of disaster incidence and damages, indicating that counties more exposed to systematic temperature fluctuations experience a higher probability and severity of weather-related losses. In Panel B, we decompose the predicted value of temperature into four components based on the four retained factors ($\hat{\lambda}_{ck}\hat{f}_{kt}$). The results imply that when systematic temperature risk, captured by higher factor realizations, increases, counties with greater exposure to these factors face higher disaster losses. Together, these findings demonstrate that systematic temperature anomaly factors, constructed independently of disaster data, capture meaningful dimensions of physical climate risk.

Given that geography is a key driver of local climate, it is plausible that some of this information may overlap with dimensions already captured by standard asset pricing factors. If so, the extracted temperature anomaly factors would load significantly onto traditional asset pricing factors, and the regressions would yield meaningful explanatory power. In Table 3, low R^2s and a lack of systematic association with the Fama-French 5 factors suggest that the temperature anomaly factors capture new information outside the span of traditional factors.

[Insert Table 3 Here]

To test whether financial markets price physical climate risk, we estimate risk premia

on temperature anomaly factors using Fama & MacBeth (1973) regressions for the cross-section of US commercial banks. Table 4 presents results. The models extend the Capital Asset Pricing Model (Sharpe, 1964; Lintner, 1965; Mossin, 1966), Fama-French 3-Factor (Fama & French, 1993), Carhart 4-Factor (Carhart, 1997), and Fama-French 5-Factor (Fama & French, 2015) Models by incorporating temperature anomaly factors.

[Insert Table 4 Here]

The results show that the second factor exhibits a marginally significant risk premium under the Fama-French 3-Factor model (–0.04, t-stat = –1.65) and the Carhart 4-Factor model (–0.05, t-stat = –1.81). Other temperature factors remain statistically insignificant, suggesting that temperature anomalies do not command an economy-wide risk premium. Temperature anomaly factors incrementally explain the variation in bank stock returns. The temperature factors increase R^2 by 31 percent, 11 percent, 10 percent, and 14 percent for the CAPM, the Fama-French 3-factor, the Carhart 4-factor, and the Fama-French 5-factor models, respectively, suggesting that these factors enhance model fit for bank stocks. The reduction in incremental R^2 from the CAPM to other models suggests that the risk associated with temperature anomaly factors is partly captured through exposures to size, value, momentum, investment, and profitability factors.

To further assess the economic relevance of temperature anomaly factors, we shift the focus from returns to their conditional volatility, recognizing that volatility is a key variable of interest in financial economics (Engle, 1982; Bollerslev, 1986). The effects of climate risk may amplify or dampen perceptions of risk over time. From an economic perspective, temperature anomaly factors may exacerbate perceived tail risks and uncertainty, leading to spikes in volatility.

Banks are both producers and consumers of financial risk, and heightened volatility in their equity prices can trigger adjustments in capital adequacy, funding costs, and lending capacity. These factors have broader implications for financial stability. To investigate how temperature anomaly factors affect volatility dynamics, we estimate a

Dynamic Conditional Correlation Multivariate Generalized Autoregressive Conditional Heteroskedasticity (DCC-MGARCH) model with exogenous variables in the variance equation. For reliable estimation, we use equally- and value-weighted returns for the *banks*, *financials*, and *insurance* industries from the Fama-French 48 industry portfolios. The complete monthly time series allows robust estimation. For each of the three industry portfolios, denoted by subscript p, the model is specified as:

$$\begin{aligned} &\Big\{ r_t = \eta + \zeta r_{mt} + \epsilon_t, \\ &\epsilon_t \sim \mathcal{N}(0, H_t) \\ &H_t = D_t R_t D_t \\ &\sigma_t^2 = \omega + \alpha \epsilon_{t-1}^2 + \beta \sigma_{t-1}^2 + \exp(\delta_0 + \sum_{k=1}^{4} \delta_k f_{kt}) \Big\}_p \end{aligned} \tag{3}$$

where r_{pt} is the excess return of portfolio, r_{mt} is the excess market return, ϵ_t is the innovation term, σ_{pt}^2 is the conditional variance, H_t is the conditional variance-covariance matrix, D_t is the conditional variance-covariance matrix $\sqrt{\sigma_{pt}^2}$, R_t is the dynamic correlation matrix, and f_{kt} are the temperature anomaly factors. Positive values of coefficients (δ_{pk}s) of interest imply volatility amplification, while negative values indicate the opposite effect.

[Insert Table 5 Here]

Table 5 shows that temperature anomaly factors affect volatility in a heterogeneous but economically meaningful way. For banks and other financial firms, the first two factors raise conditional volatility, consistent with markets viewing broad climatic variability as a source of uncertainty for institutions whose portfolios, loan books, and counterparty exposures are sensitive to macroeconomic disruptions. These effects are concentrated in equally weighted portfolios. In Panel B of Table 5, when we shift to value-weighted specifications, the loadings on temperature factors largely disappear. This attenuation is intuitive: large, diversified banks spread their climate-related exposures across regions and sectors, thereby diluting the impact of localized shocks

on volatility. Equally weighted portfolios, in contrast, place relatively more weight on smaller and likely regionally concentrated institutions. The amplification is most evident among smaller banks with limited diversification, indicating a source of fragility that is less apparent in larger banks. This asymmetry highlights the significance of volatility as a mechanism through which climate shocks can impact financial stability.

3.2 Estimating systemic physical climate risk

3.2.1 Estimating climate betas

In this section, we estimate temperature anomaly betas, *climate betas*, which serve as a forward-looking measure of bank-specific exposure to the physical climate risk, following the approach of Jung et al. (2025). We construct mimicking portfolios for the temperature anomaly factors $\{f_{kt}\}_{k=1}^{4}$ using all US stocks from CRSP. For each stock, we estimate betas using 48-month rolling-window regressions, where excess stock returns are regressed on the market factor and the four temperature anomaly factors. We then sort stocks into quintiles based on their estimated betas for each temperature anomaly factor. We form market-cap weighted mimicking portfolios by taking a long position in the top quintile and a short position in the bottom quintile. Constructing these factor-mimicking portfolios is necessary for interpreting climate risk and stress scenarios, as directly using factor scores introduces ambiguity in defining 'stress' when estimating physical climate risk.

We estimate banks' betas, $(\beta_{b,k})$, with respect to temperature anomaly factors as follows:

$$r_{bt} = \alpha_b + \beta_{b,Mkt}\text{Mkt}_t + \sum_{k=1}^{4} \beta_{b,k}\mathbb{P}_{f_k t} + u_{bt}. \tag{4}$$

Here, Mkt_t represents the excess market return, capturing market conditions. We estimate this model using a 48-month rolling window regression, allowing for temporal variation in banks' exposures to temperature anomaly factors. Including the market risk premium controls for systematic market-wide movements ensures that general market

fluctuations do not confound the exposures.

Table C.2 summarizes the distribution of estimated climate betas for US banks. Climate betas vary across institutions and within institutions over time. This pattern implies that banks' exposure to temperature anomaly factors has a panel structure. On average, banks exhibit negative sensitivity to the first and fourth temperature-anomaly factors and positive sensitivity to the second, but the substantial within-bank dispersion indicates that exposures evolve materially over time.

Figure 4 compares each bank's estimated climate beta with the deposit-weighted average county loading on the corresponding temperature-anomaly factor. The positive association for the two dominant factors indicates that banks whose funding is concentrated in counties more exposed to systematic temperature variability also exhibit higher market-based climate betas. The third factor shows no clear pattern, while the fourth remains weakly positive. This alignment provides an out-of-sample validation. The temperature anomaly-based factors and market-based betas are estimated independently of bank balance-sheet information, yet they co-move in the expected direction. Because county loadings are time-invariant but deposit shares evolve, the relationship reflects how shifts in banks' geographic footprint translate into changes in measured exposures. These patterns are complementary to recent evidence that local abnormal temperatures affect the allocation of bank deposits, reflecting climate-related behavioral responses by depositors (Dursun-de Neef & Ongena, 2024).

[Insert Figure 4 Here]

In Table C.3, we examine how banks' climate betas are associated with bank characteristics. Larger banks exhibit lower exposure to the first temperature-anomaly factor. Conditional on size, banks with more geographically dispersed deposits (higher deposit entropy (Gandhi et al., 2024)) have greater exposure to that factor, as broader presence increases contact with systematically exposed regions. Better-capitalized banks display higher betas to the second factor. This suggests that high bank capital enables banks to

absorb and potentially intermediate climate risk rather than withdrawing from those markets. Overall, geographic exposures explain where climate risk enters bank balance sheets, while structural characteristics explain how it is managed across institutions.

3.2.2 Estimating systemic physical climate risk

Following Jung et al. (2025), we define physical climate risk for a bank as follows:

$$\text{Physical Climate Risk}_{bt} = lD_{bt} - (1-l)\big[E_{bt}(exp(\beta_{b,kt}\log(1-\theta)))\big]. \tag{5}$$

In equation 5, l represent capital ratio (set to 8 percent), D_{bt} is bank b's liabilities, E_{bt} represents bank b's market equity at time t, and θ represents the stress level, set to -60 percent. Figure 5 depicts the temporal and cross-sectional dynamics of physical climate risk exposures.

[Insert Figure 5 Here]

Figure 5 summarizes both the cross-sectional range (shaded area) and the average exposure (solid line) from 1990 to 2019. Over the sample period, physical climate risk remains mostly negative. These estimates indicate that banks, on average, hold sufficient capital to absorb physical climate-related shocks. However, the breadth of exposures varies significantly over time. The period from 2005 to 2010 is marked by an increase in the cross-sectional range. After 2010, both the dispersion and average level of physical climate risk stabilize, consistent with sector-wide adjustments such as enhanced risk management, portfolio reallocation, or evolving regulatory responses and attention to climate change. Figure 5 thus highlights two key patterns: climate-related exposures vary substantially across banks and tend to rise during periods of financial and climate stress. However, on average, banks have maintained capital buffers sufficient to absorb physical climate risk over the sample period.

Next, we estimate systemic physical climate risk as follows:

$$\text{Systemic Physical Climate Risk}_t = \sum_b \text{Physical Climate Risk}_{bt}^{+}. \tag{6}$$

In equation 6, the superscript '+' denotes positive values of physical climate risk, capturing the cumulative under-capitalization risk posed by climate-specific stress events. This measure highlights the contribution of at-risk institutions to systemic physical climate risk.

[Insert Figure 6 Here]

Figure 6a presents the time series of systemic physical climate risk. The magnitude of systemic risk reaches approximately 500 billion dollars during the sample period, and the series displays three distinct peaks: in 2005, 2012, and 2018–2019. These peaks coincide with notable periods of climate stress, and, as shown in Figure 6b, appear to be driven by different temperature anomaly factors. The 2005 spike aligns with Hurricane Katrina and an active Atlantic hurricane season, showing concentrated exposures in affected regions. The 2012 peak coincides with Hurricane Sandy. The sustained rise in 2018–2019 reflects consecutive years of record-breaking heat, increasing physical climate stress in the US banking sector.

It is important to note that disaster damages, insured losses, or direct measures of physical destruction are not inputs to the temperature anomaly factors or systemic risk estimation. The model relies solely on bank-level exposures to the former. The close alignment between estimated systemic risk peaks and major climate events provides supporting evidence that the climate betas capture economically meaningful variation in physical climate risk. While factor analysis provides a parsimonious way to summarize systematic climate variability, it comes with the familiar challenge of rotational indeterminacy. This is not an operational limitation for estimating systemic physical climate risk, since the space spanned by the factors is uniquely identifiable and sufficient to capture common variation. For completeness, in Appendix A, we address this issue

directly by constructing location-based temperature anomaly factors using geographic coordinates as pre-specified loadings.

These estimates, limited to listed banks only, amount to approximately 25 percent of total US bank equity as of 2019:Q4 reported by all banks to the FFIEC. As climate-related shocks can exhibit non-linearities through asset repricing, insurance spillovers, and supply chain disruptions, these numbers likely represent lower bounds of systemic physical risk exposure. The evolution of systemic physical climate risk indicates that physical climate shocks, though localized in origin, can aggregate into significant sector-wide vulnerabilities. These findings underscore the case for incorporating physical climate risk into prudential regulation.

3.3 Implications for bank lending

Having demonstrated the usefulness of temperature anomaly factors in capturing systematic physical climate risk and contributing to systemic exposures, we now examine their actual effects. Specifically, we test whether banks more exposed to temperature anomalies adjust their lending to small businesses. Our analysis is necessarily limited to banks for which we can estimate climate betas, but these institutions account for a substantial share of the US banking sector. Small firms provide a natural laboratory for this test. They are bank-dependent, geographically concentrated, and lack the ability to hedge or diversify local climate shocks. If banks with higher exposure to temperature anomaly factors reduce credit supply, this would provide direct evidence that physical climate risk transmits into the real economy through the lending channel and would reinforce the validity of the systemic risk estimates in the previous section.

We proceed by ascribing an economic meaning to the first factor, which alone explains more than 59 percent of the variation in temperature anomalies across contiguous US counties. In Figure 7, we present a time series of Factor 1 scores and a time series of the cross-sectional average of temperature anomalies across 3,108 contiguous US counties. The near-perfect correlation (98.71 percent) suggests that the first factor effectively captures the aggregate dimension of temperature variability. Because counties'

exposure to it is nearly uniformly positive, the first factor captures the common warming dimension of physical climate variability. A bank's beta with respect to this factor, therefore, measures its exposure to the aggregate component of physical climate risk: higher anomalies correspond to greater exposure, and more-exposed banks should scale back lending.

To test whether and how banks' exposures to the first factor correlate with small business lending, we employ the following regression specification:

$$\begin{aligned}\text{Lending Outcome}_{cbt} =& \gamma_1 \text{Bank Exposure}_{bt-1} + \Gamma' \text{Controls}_{bt-1} \\ &+ \text{Bank}_b \times \text{County}_c + \text{County}_c \times \text{Year}_t + \upsilon_{cbt}.\end{aligned} \tag{7}$$

In equation (7), the subscripts c, b, and t represent county, bank, and year, respectively. The dependent variable is the logarithm of either the number or the total volume of small business loan originations by bank b in county c during year t. The key independent variable, bank exposure, is measured as the calendar-year average of bank b's loading on the first temperature anomaly factor, $\beta_{b,k=1}$, estimated in equation (4). We include standard bank-level controls to account for differences in balance sheet strength and risk-taking capacity. These controls are: size (log of total assets), capitalization (equity-to-assets ratio), profitability (operating income-to-assets ratio), and loan quality (non-performing loans-to-assets ratio). Standard errors are clustered by both county and bank. We report descriptive statistics of all relevant variables in Table C.1.

Equation (7) has two sets of fixed effects. The county-year fixed effects imply a transformation that corresponds to asking whether small businesses in a county experience a larger reduction in lending from a bank with relatively high exposure to the first temperature anomaly factor. Because the comparison is made within the same county-year, county-specific demand shocks and other sources of local heterogeneity are absorbed by the county-year fixed effects (Gilje et al., 2016; Cortés & Strahan, 2017). As small businesses rely on local lenders, and banks may favor some borrowers based on long-standing relationships, collateral quality, or historical creditworthiness, we include county-bank fixed effects control for the endogenous matching between small

businesses within a county and banks.

[Insert Table 6 Here]

Table 6 reports the effect of banks' exposures to the dominant temperature anomaly factor on small business lending. Across columns (1)–(4), higher exposures are consistently associated with lower credit supply. In columns (1) and (2), the dependent variable is the logarithm of the number of originations. On average, a bank makes about 9 small business loans per county–year. In columns (1) and (2), the coefficient estimates are –0.34 and –0.20, respectively. Economically, these coefficients imply 1–2 fewer small business loan origination with a standard deviation (0.843) increase in a bank's exposure to the first factor. Columns (3) and (4) use loan volume as the dependent variable. The mean loan volume is approximately 360 thousand dollars. A standard deviation increase in exposure is associated with a reduction of 9–19 percent, or 32.4–67.9 thousand dollars. Including bank-level controls again reduces the magnitude, but the key coefficient remains statistically significant and economically meaningful. These results indicate that banks more exposed to temperature anomalies reduce credit to small businesses, both in the number and amount of loans. This evidence reinforces the view that temperature anomaly factors capture meaningful climate exposures with real consequences for credit supply.

The effect of climate exposures on lending may depend on the strength of a bank's local presence. A branch network not only signals a commitment to serve a market but also enables banks to develop borrower relationships, accumulate local knowledge, and reduce information frictions. In markets where a bank maintains branches, it has a greater scope to screen borrowers, monitor loans, and preserve long-term relationships. By contrast, in markets without a branch presence, lending is more transactional, and banks may respond more aggressively to heightened climate risk by cutting back credit.

[Insert Table 7 Here]

To test this idea, we follow Cortés & Strahan (2017) and classify each county as either a core market, where a focal bank has a branch, or a non-core market, where a focal bank lacks a local branch. Table 7 reports the results. The baseline negative effect of exposure to average temperature anomaly on lending is concentrated in non-core markets, while it is muted in core markets. In odd-numbered columns, we hold all factors that determine credit availability fixed across the two county groups. In even-numbered columns, we relax this restriction and we interact all bank controls and fixed effects with the non-core county dummy. Overall, we find that the baseline negative correlation between credit availability to small businesses and banks' exposure to the average temperature anomaly factor is more discernible in non-core markets.

This pattern highlights the significance of the branch network and suggests that geographic reach is crucial for how banks transmit climate risk to their credit supply. Lending relationships anchored by a branch presence appear more resilient, consistent with the notion that banks protect informational rents and maintain established relationships where they have invested in local expertise. In contrast, in markets where relationships are weaker, banks adjust credit supply more readily in response to climate exposures.

A bank with more volatile equity returns may appear to have a higher climate beta even if its true exposure to the temperature factor is unchanged. To address the concern that estimated betas may mechanically scale with bank return volatility, we augment the baseline specification with the bank's realized stock-return volatility, measured as squared excess returns, and present the results in Table C.4. Controlling for volatility isolates banks' sensitivity to the climate factor from general riskiness. The results remain quantitatively and qualitatively similar, indicating that the main findings of this section are not driven by high-volatility banks but reflect meaningful differences in climate exposure. Hence, the lending response to climate exposure persists even after accounting for differences in banks' return variability.

3.4 Estimating physical climate risk using global temperature data

In the previous section, we estimate temperature anomaly factors using temperature data for contiguous US counties. Given that climate change is a global phenomenon, recent research emphasizes that global temperature shocks have distinct and far-reaching macroeconomic consequences. Bilal & Känzig (2024) show that an increase in global average temperature is one of the key drivers of GDP losses, extreme climatic events, and broader financial instability. Additionally, local weather patterns are partly shaped by global climate dynamics (IPCC, 2012; Wallace & Hobbs, 2006; Trenberth et al., 2007), raising the possibility that systemic climate risk in the US banking sector may also reflect global temperature anomalies. This 'local versus global' distinction is relevant for large US banks. On the one hand, US banks operate globally and are thus exposed to global phenomena with significant macroeconomic implications (Goldberg, 2009; Cetorelli & Goldberg, 2012; V. Bruno & Shin, 2015a,b). On the other hand, US banks' exposures may reflect domestic conditions, given that their loan portfolios, regulatory oversight, and day-to-day operations are concentrated within national borders. Whether global temperature anomalies meaningfully contribute to systemic physical climate risk beyond local factors is therefore an empirical question.

In Appendix B, we incorporate global temperature anomaly factors to assess whether global climate variability adds a layer of risk exposure for US banks. We find that local and global temperature anomaly factors do not have a 1-to-1 relationship. Global climate variation can heighten US systemic risk, likely indirectly and during periods of financial stress.

4 Conclusion

This paper estimates US banks' exposure to physical climate risk using temperature-anomaly factors derived via factor analysis. These factors provide a data-driven approach to summarize systematic climate variability. We find that temperature anomaly factors capture meaningful dimensions of physical climate risk. They are correlated with disaster-related damage, distinct from standard asset-pricing factors, and pro-

vide insights into the volatility of bank stocks. The systemic physical risk is sizeable, with peaks approaching 500 billion dollars. Banks that are more sensitive to temperature anomalies tend to reduce lending to small businesses, and these effects are most pronounced in markets without a physical branch presence.

Our framework makes three contributions. It shows that climate risk exposures can be quantified without relying on incomplete firm disclosures; provides a consistent, forward-looking measure of systemic physical risk; and offers a way to connect climate variability to financial outcomes and the real economy. These findings extend the climate finance literature beyond transition risk and event-driven studies, highlighting the role of ongoing temperature variability in financial fragility.

For regulators and policymakers, the implications are direct. Physical climate risk is not just a long-run environmental concern but a measurable, near-term source of systemic financial risk. Incorporating such exposures into capital regulation, stress tests, and risk management practices will be essential as climate variability intensifies. Our estimates likely understate the true scale of potential losses because they exclude feedback effects from insurance, asset repricing, or supply chain disruptions. Hence, these estimates are a conservative benchmark. The evidence highlights the need for supervisory frameworks that account for physical climate risk.

References

Abedifar, P., Kashizadeh, S. J., & Ongena, S. (2024). Flood, farms and credit: The role of branch banking in the era of climate change. *Journal of Corporate Finance*, 102544.

Acharya, V., Engle, R., & Pierret, D. (2014). Testing macroprudential stress tests: The risk of regulatory risk weights. *Journal of Monetary Economics*, *65*, 36-53.

Acharya, V., Engle, R., & Richardson, M. (2012). Capital shortfall: A new approach to ranking and regulating systemic risks. *American Economic Review*, *102*(3), 59-64.

Acharya, V. V., Brownlees, C., Engle, R., Farazmand, F., & Richardson, M. (2013). Measuring systemic risk. In *Managing and measuring risk: Emerging global standards and regulations after the financial crisis* (pp. 65–98). World Scientific.

Acharya, V. V., Johnson, T., Sundaresan, S., & Tomunen, T. (2022). *Is physical climate risk priced? evidence from regional variation in exposure to heat stress* (Tech. Rep.). National Bureau of Economic Research.

Altavilla, C., Boucinha, M., Pagano, M., & Polo, A. (2024). Climate risk, bank lending and monetary policy. *Available at SSRN: https://ssrn.com/abstract=4918451*.

Baele, L., De Jonghe, O., & Vander Vennet, R. (2007). Does the stock market value bank diversification? *Journal of Banking & Finance*, *31*(7), 1999–2023.

Battiston, S., Mandel, A., Monasterolo, I., Schütze, F., & Visentin, G. (2017). A climate stress-test of the financial system. *Nature Climate Change*, *7*(4), 283-288.

BCBS. (2021). *Climate-related risk drivers and their transmission channels* (Tech. Rep.). Basel Committee on Banking Supervision, Bank for International Settlements.

BCBS. (2022a). *Frequently asked questions on climate-related financial risks* (Tech. Rep.). Basel Committee on Banking Supervision, Bank for International Settlements.

BCBS. (2022b). *Principles for the effective management and supervision of climate-related financial risks* (Tech. Rep.). Basel Committee on Banking Supervision, Bank for International Settlements.

Benincasa, E., Kabas, G., & Ongena, S. (2025). "There is no planet B", but for banks "There are countries B to Z": Domestic climate policy and cross-border lending. *Available at SSRN:https://ssrn.com/abstract=4075737*.

Beyene, W., De Greiff, K., Delis, M. D., & Ongena, S. (2024). Too-big-to-strand? bond versus bank financing in the transition to a low-carbon economy. *Available at SSRN:https://ssrn.com/abstract=3960296*.

Bilal, A., & Känzig, D. R. (2024). *The macroeconomic impact of climate change: Global vs. local temperature* (Tech. Rep.). National Bureau of Economic Research.

Blickle, K., Hamerling, S. N., & Morgan, D. P. (2021). How bad are weather disasters for banks? *Available at SSRN: https://ssrn.com/abstract=3961081*.

Blickle, K., Morse, A., & Sastry, P. (2025). Banks as stewards. *Work. Pap., New York Federal Reserve Bank*.

BoE. (2021). *Climate-related financial risk management and the role of capital requirements* (Tech. Rep.). Bank of England Prudential Regulatory Authority.

BoE. (2022). *Results of the 2021 climate biennial exploratory scenario* (Tech. Rep.). Bank of England.

BoE. (2023). *Report on climate-related risks and the regulatory capital frameworks* (Tech. Rep.). Bank of England.

Bollerslev, T. (1986). Generalized autoregressive conditional heteroskedasticity. *Journal of Econometrics*, *31*(3), 307-327.

Bolton, P., & Kacperczyk, M. (2021). Do investors care about carbon risk? *Journal of financial economics*, *142*(2), 517-549.

Brownlees, C., & Engle, R. F. (2017). Srisk: A conditional capital shortfall measure of systemic risk. *The Review of Financial Studies*, *30*(1), 48-79.

Bruno, B., & Lombini, S. (2023). Climate transition risk and bank lending. *Journal of Financial Research*, *46*, S59-S106.

Bruno, V., & Shin, H. S. (2015a). Capital flows and the risk-taking channel of monetary policy. *Journal of Monetary Economics*, *71*, 119-132.

Bruno, V., & Shin, H. S. (2015b). Cross-border banking and global liquidity. *Review of Economic Studies*, *82*(2), 535-564.

Carattini, S., Heutel, G., Melkadze, G., & Mourelon, I. (2025). Transition risk: Sources and policy responses. *Available at SSRN:https://ssrn.com/abstract=5069455*.

Carhart, M. M. (1997). On persistence in mutual fund performance. *Journal of Finance*, *52*(1), 57-82.

Cetorelli, N., & Goldberg, L. S. (2012). Banking globalization and monetary transmission. *Journal of Finance*, *67*(5), 1811-1843.

Cicco, V. D., Gschossmann, I., & Kok, C. (2025). Bank lending implications of climate stress tests. *Available at SSRN:https://ssrn.com/abstract=5382449*.

Connor, G., & Korajczyk, R. A. (1988). Risk and return in an equilibrium APT: Application of a new test methodology. *Journal of Financial Economics*, *21*(2), 255-289.

Correa, R., He, A., Herpfer, C., & Lel, U. (2022). The rising tide lifts some interest rates: Climate change, natural disasters, and loan pricing. *Available at SSRN: https://ssrn.com/abstract=4161300*.

Cortés, K. R., & Strahan, P. E. (2017). Tracing out capital flows: How financially integrated banks respond to natural disasters. *Journal of Financial Economics*, *125*(1), 182-199.

Degryse, H., Goncharenko, R., Theunisz, C., & Vadasz, T. (2023). When green meets green. *Journal of Corporate Finance*, *78*, 102355.

Delis, M. D., Greiff, K. d., Iosifidi, M., & Ongena, S. (2019). Being stranded with fossil fuel reserves? climate policy risk and the pricing of bank loans. *Financial Markets, Institutions & Instruments*.

Duan, T., Li, F. W., & Wen, Q. (2025). Is carbon risk priced in the cross section of corporate bond returns? *Journal of Financial and Quantitative Analysis*, *60*(1), 1-35.

Dursun-de Neef, O., & Ongena, S. (2024). Climate change and bank deposits. *Available at SSRN: https://ssrn.com/abstract=4657847*.

ECB. (2020). *Guide on climate-related and environmental risks: Supervisory expectations relating to risk management and disclosure* (Tech. Rep.). European Central Bank.

ECB. (2022a). *Ecb sets deadlines for banks to deal with climate risks* (Tech. Rep.). European Central Bank.

ECB. (2022b). *Good practices for climate-related and environmental risk management: Observations from the 2022 thematic review* (Tech. Rep.). European Central Bank.

Engle, R. F. (1982). Autoregressive conditional heteroscedasticity with estimates of the variance of united kingdom inflation. *Econometrica*, 987-1007.

Fama, E. F., & French, K. R. (1993). Common risk factors in the returns on stocks and bonds. *Journal of Financial Economics*, *33*(1), 3-56.

Fama, E. F., & French, K. R. (2015). A five-factor asset pricing model. *Journal of financial economics*, *116*(1), 1–22.

Fama, E. F., & MacBeth, J. D. (1973). Risk, return, and equilibrium: Empirical tests. *Journal of Political Economy*, *81*(3), 607-636.

Gandhi, P., Palia, D., & Pan, J. (2024). Do "MEASURES" of bank diversification measure up? *Available at SSRN: https://ssrn.com/abstract=4952789*.

Giannetti, M., Jasova, M., Loumioti, M., & Mendicino, C. (2023). Glossy green banks: The disconnect between environmental disclosures and lending activities. *Available at SSRN: https://ssrn.com/abstract=4668588*.

Gilje, E. P., Loutskina, E., & Strahan, P. E. (2016). Exporting liquidity: Branch banking and financial integration. *Journal of Finance*, *71*(3), 1159-1184.

Goldberg, L. S. (2009). Understanding banking sector globalization. *IMF Staff Papers*, *56*(1), 171-197.

Green, D., & Vallee, B. (2024). Measurement and effects of bank exit policies. *Available at SSRN: https://ssrn.com/abstract=4090974*.

Haushalter, D., Henry, J. J., & Iliev, P. (2023). Can banks save mountains? *Review of Corporate Finance Studies*, *12*(4), 761-791.

Hsiang, S. (2016). Climate econometrics. *Annual Review of Resource Economics*, *8*(1), 43-75.

IPCC. (2001). *Climate change 2001: The scientific basis*. Cambridge University Press, Cambridge.

IPCC. (2012). *Managing the risks of extreme events and disasters to advance climate change adaptation: Special report of the intergovernmental panel on climate change*. Cambridge University Press.

Ivanov, I. T., Kruttli, M. S., & Watugala, S. W. (2024). Banking on carbon: Corporate lending and cap-and-trade policy. *Review of Financial Studies*, *37*(5), 1640-1684.

Jourde, T., & Moreau, Q. (2024). Systemic climate risk. *Available at SSRN: https://ssrn.com/abstract=4300469*.

Jung, H., Engle, R., Ge, S., & Zeng, X. (2024). Physical climate risk factors and an application to measuring insurers' climate risk exposure. *FRB of New York Staff Report No. 1066*.

Jung, H., Engle, R. F., & Berner, R. (2025). Crisk: measuring the climate risk exposure of the financial system. *Journal of Financial Economics*, *171*, 104076.

Jung, H., Santos, J. A., & Seltzer, L. (2024). *US banks' exposures to climate transition risks* (Tech. Rep.).

Kacperczyk, M. T., & Peydró, J.-L. (2022). Carbon emissions and the bank-lending channel. *Available at SSRN: https://ssrn.com/abstract=3915486*.

Kim, S., Kumar, N., Lee, J., & Oh, J. (2025). Esg lending. *Journal of Financial Economics*, *173*, 104150.

Klomp, J. (2014). Financial fragility and natural disasters: An empirical analysis. *Journal of Financial Stability*, *13*, 180-192.

Koetter, M., Noth, F., & Rehbein, O. (2020). Borrowers under water! rare disasters, regional banks, and recovery lending. *Journal of Financial Intermediation*, *43*, 100811.

Kousky, C., Kunreuther, H., LaCour-Little, M., & Wachter, S. (2020). Flood risk and the us housing market. *Journal of Housing Research*, *29*(sup1), S3–S24.

Kruttli, M. S., Roth Tran, B., & Watugala, S. W. (2024). Pricing poseidon: Extreme weather uncertainty and firm return dynamics. *Available at SSRN: https://ssrn.com/abstract=3284517*.

Li, L., Li, X., Ongena, S., & Wang, Y. (2025). Extreme rainfall and municipal financing: Risk pricing and adaptive mitigation by sponge cities. *Available at SSRN: https://ssrn.com/abstract=5169333*.

Lintner, J. (1965). Security prices, risk, and maximal gains from diversification. *Journal of Finance*, *20*(4), 587-615.

Morse, A., & Sastry, P. (2025). The economics of net zero banking. *Annual Review of Financial Economics*, *17*(1), 343–361.

Mossin, J. (1966). Equilibrium in a capital asset market. *Econometrica*, 768-783.

Nguyen, D. D., Ongena, S., Qi, S., & Sila, V. (2022). Climate change risk and the cost of mortgage credit. *Review of Finance*, *26*(6), 1509-1549.

Pástor, L., Stambaugh, R. F., & Taylor, L. A. (2021). Sustainable investing in equilibrium. *Journal of Financial Economics*, *142*(2), 550-571.

Rajan, R., & Ramcharan, R. (2023). *Finance and climate resilience: Evidence from the long 1950s us drought* (Tech. Rep.). National Bureau of Economic Research.

Roll, R., & Ross, S. A. (1980). An empirical investigation of the arbitrage pricing theory. *Journal of Finance*, *35*(5), 1073-1103.

Roncoroni, A., Battiston, S., Escobar-Farfán, L. O., & Martinez-Jaramillo, S. (2021). Climate risk and financial stability in the network of banks and investment funds. *Journal of Financial Stability*, *54*, 100870.

Sastry, P. (2022). Who bears flood risk? Evidence from mortgage markets in Florida. *Available at SSRN: https://ssrn.com/abstract=4306291*.

Sastry, P., Sen, I., & Tenekedjieva, A.-M. (2024). When insurers exit: Climate losses, fragile insurers, and mortgage markets. *Available at SSRN: https://ssrn.com/abstract=4674279*.

Sastry, P., Verner, E., & Marques Ibanez, D. (2024). Business as usual: Bank net zero commitments, lending, and engagement. *Available at SSRN: https://ssrn.com/abstract=4825987*.

Sharpe, W. F. (1964). Capital asset prices: A theory of market equilibrium under conditions of risk. *Journal of Finance*, *19*(3), 425-442.

TCFD. (2017). *Recommendations of the task force on climate-related financial disclosures* (Report). Financial Stability Board.

Trenberth, K. E., Jones, P. D., Ambenje, P., Bojariu, R., Easterling, D., Klein Tank, A., ... others (2007). Observations. surface and atmospheric climate change. chapter 3.

Vander Vennet, R. (1996). The effect of mergers and acquisitions on the efficiency and profitability of ec credit institutions. *Journal of Banking & Finance*, *20*(9), 1531–1558.

Vennet, R. V. (2002). Cost and profit efficiency of financial conglomerates and universal banks in europe. *Journal of Money, Credit and Banking*, 254–282.

Wallace, J. M., & Hobbs, P. V. (2006). *Atmospheric science: An introductory survey* (Vol. 92). Elsevier.

Table 1: **Factor analysis of temperature anomaly across US counties**

This table presents the output of factor analysis implemented on the county-month-year level temperature anomaly for US counties. Here, temperature anomaly, denoted $\Delta\mathbb{T}_{cmy} = \mathbb{T}_{cmy} - \frac{1}{30}\sum_{y=1951}^{1980}\mathbb{T}_{cmy}$. The subscripts c, m, and y represent county, month, and year, respectively. The temperature data from the Climate Research Unit of the University of East Anglia. In Panel A, we present the eigenvalues of the first four factors and the proportion of the total variation in monthly temperature anomaly across US counties. The sample period spans 36 years (1984:M1–2019:M12). In Panel B, we present summary statistics of factor loadings estimated for 3,108 US counties.

Panel A: Factor analysis output

Factor	Eigenvalue	Difference	Variance explained:	
			Proportion	Cumulative
Factor 1	1,860.200	1,332.197	0.599	0.599
Factor 2	528.003	266.313	0.170	0.768
Factor 3	261.690	149.579	0.084	0.853
Factor 4	112.111	28.747	0.036	0.889

Panel B: Summary statistics – County loadings (N = 3,108)

	Mean	SD	p25	p75
County loading - Factor 1	0.731	0.254	0.697	0.888
County loading - Factor 2	0.081	0.404	-0.282	0.459
County loading - Factor 3	0.030	0.289	-0.226	0.254
County loading - Factor 4	0.041	0.186	-0.099	0.150

Table 2: **Local factor scores and loadings, and natural disasters**
This table presents the validation results for the latent factors and their loadings estimated via factor analysis of county-level monthly temperature anomalies. The dependent variables correspond to one-period-ahead disaster occurrences and their intensities. In column (1), the dependent variable is *Disaster*, a dichotomous variable that equals 1 (0 otherwise) if the reported total damages within SHELDUS are positive. In columns (2)-(4), the dependent variables are the logarithm of inflation-adjusted (to the 2022 level) per capita crop, property, and total damages, respectively. The data are monthly panel and the sample period is from 1984 to 2019. The standard errors are clustered by county and t-statistics are in parentheses. Significance: * $p < 0.10$, ** $p < 0.05$, *** $p < 0.01$.

	(1)	(2)	(3)	(4)
	Dependent variable:			
	Disaster (1=Yes, 0 = No)	Ln(· Damages) | Disaster = 1		
		Crop	Property	Total
Panel A				
Predicted temperature anomaly	0.0082***	0.0457***	0.0213***	0.0524***
	(9.5922)	(11.1296)	(4.1821)	(8.8969)
Residual temperature anomaly	-0.0060***	-0.0118***	-0.0327***	-0.0277***
	(-9.5513)	(-3.5298)	(-8.5590)	(-6.1082)
R^2	0.1236	0.2092	0.1881	0.2270
Panel B				
County loading - Factor 1 × Factor 1 scores	0.0072***	0.0402***	0.0558***	0.0837***
	(4.5545)	(4.8760)	(5.7986)	(7.1236)
County loading - Factor 2 × Factor 2 scores	0.0087***	0.0310***	0.0272***	0.0438***
	(9.0530)	(5.7532)	(4.0720)	(5.8330)
County loading - Factor 3 × Factor 3 scores	0.0144***	0.0968***	0.0344***	0.0967***
	(9.4949)	(13.5595)	(3.5441)	(8.7302)
County loading - Factor 4 × Factor 4 scores	-0.0060***	-0.0235*	-0.0912***	-0.0813***
	(-2.5900)	(-1.7868)	(-6.4609)	(-4.6436)
Residual temperature anomaly	-0.0062***	-0.0117***	-0.0344***	-0.0289***
	(-9.9257)	(-3.4986)	(-8.9561)	(-6.3590)
R^2	0.1237	0.2095	0.1883	0.2273
N	1,339,548	290,208	290,208	290,208
County FE	✓	✓	✓	✓
Year × Month FE	✓	✓	✓	✓

Table 3: **Temperature anomaly and traditional factors: Time-series regressions**
This table reports time-series regressions of the extracted local climate anomaly factors on the Fama–French five factors (Market, SMB, HML, RMW, and CMA). The dependent variables are the monthly scores of the first four local factors. Standard errors are Newey–West corrected with 12 lags. The sample covers 432 months from January 1984 to December 2019.

	(1)	(2)	(3)	(4)
	Dependent variable: Factor scores			
	Factor 1	Factor 2	Factor 3	Factor 4
Market	-0.008	0.001	-0.010	-0.010
	(-0.670)	(0.038)	(-0.798)	(-0.800)
SMB	0.025	-0.005	-0.022	-0.010
	(1.288)	(-0.285)	(-1.337)	(-0.516)
HML	0.016	-0.009	-0.041*	-0.004
	(0.832)	(-0.334)	(-1.770)	(-0.176)
RMW	-0.011	-0.052*	-0.036	-0.004
	(-0.459)	(-1.952)	(-1.616)	(-0.189)
CMA	-0.070**	0.049	0.024	-0.052
	(-2.557)	(1.280)	(0.655)	(-1.571)
N	432	432	432	432
R^2	0.018	0.019	0.019	0.011

Table 4: **Physical risk pricing and incremental explanatory power of temperature anomaly factors**

This table presents results from Fama-MacBeth regressions on the cross-section of US commercial bank returns. Commercial banks are identified as firms with a *siccd* value of 70 or *hsiccd* value of 6712. The table reports risk premiums for the first four temperature factors, derived from factor analysis of county-level monthly temperature anomaly data, in models that augment traditional asset pricing frameworks, including the CAPM, Fama-French 3-Factor, Carhart 4-Factor, and Fama-French 5-Factor models. It also reports R^2 values for the original and augmented models to assess the incremental explanatory power of temperature factors. The standard errors are Newey-West corrected for 12 lags, and t-statistics are in parentheses. The sample includes 1,231 commercial bank stocks in Panel B over 432 months (1984:M1 – 2019:M12). Significance levels: * $p < 0.10$, ** $p < 0.05$, *** $p < 0.01$.

	(1)	(2)	(3)	(4)
	Traditional model augmented with temperature anomaly factors			
	CAPM	FF 3-Factor	Carhart 4-Factor	FF 5-Factor
Factor 1	0.005	0.018	0.025	0.015
	(0.160)	(0.515)	(0.702)	(0.421)
Factor 2	-0.034	-0.043*	-0.052*	-0.012
	(-1.398)	(-1.651)	(-1.814)	(-0.445)
Factor 3	0.037	0.049	0.054	0.052
	(1.164)	(1.472)	(1.626)	(1.395)
Factor 4	0.007	0.015	0.019	0.012
	(0.332)	(0.654)	(0.810)	(0.515)
R^2 – Augmented model	0.314	0.508	0.527	0.492
R^2 – Original model	0.003	0.393	0.428	0.356
ΔR^2 – Augmented minus original	0.311	0.115	0.099	0.136
N	1,231	1,231	1,231	1,231
T	431	431	431	431

Table 5: **Temperature anomaly factors and conditional volatility of banks and financials**

This table reports the results from Dynamic Conditional Correlation Multivariate GARCH (DCC-MGARCH) models estimated on monthly returns of Fama-French industry portfolios classified as Banks and Financials over the sample period 1984:M1 to 2019:M12. Each column presents results for alternative specifications of the mean equation, using the CAPM (Column 1), the Fama-French 3-Factor (Column 2), the Carhart 4-Factor (Column 3), and the Fama-French 5-Factor model (Column 4). The upper panel presents the variance equation estimates. For each portfolio, the table reports the coefficients for the temperature anomaly factors($\delta_k s$), along with the ARCH (α) and the GARCH (β) parameters. The middle panel presents the estimated DCC parameters. The parameters λ_1 and λ_2 govern the evolution of the dynamic conditional correlation between the two industries over time, where the former captures the sensitivity to lagged standardized residuals, and the latter captures the persistence of past conditional correlations. The table also reports the average conditional correlation (ρ) between Banks and Financials estimated over the sample period. The z-statistics are reported in parentheses. The bottom panel reports the log-likelihood values for each model specification. These values can be used to compare model fit across different mean specifications.

	(1)			(2)			(3)			(4)		
	CAPM			FF 3-Factor			Carhart 4-Factor			FF 5-Factor		
	Banks	Financials	Insurance	Banks	Financials	Insurance	Banks	Financials	Insurance	Banks	Financials	Insurance
Panel A: Equally-Weighted Portfolios												
Variance Equation												
δ_1	0.270**	0.141**	-0.039	0.252	0.797**	-0.106	0.251	0.724**	-0.159	0.298*	0.773***	-0.119
	(2.383)	(2.003)	(-0.178)	(1.630)	(5.071)	(-0.433)	(1.588)	(3.688)	(-0.636)	(1.778)	(4.15)	(-0.481)
δ_2	0.294**	0.194**	-0.285	0.594*	0.064	-0.242	0.641**	0.114	-0.274	0.654**	0.268	-0.268
	(2.092)	(2.020)	(-1.599)	(1.842)	(0.425)	(-1.163)	(2.231)	(0.593)	(-1.336)	(2.15)	(0.882)	(-1.303)
δ_3	-0.357***	-0.116	0.216	-0.557***	0.201	0.293	-0.536***	0.275	0.334	-0.567***	0.362	0.266
	(-2.821)	(-1.645)	(0.67)	(-3.173)	(1.236)	(1.176)	(-3.118)	(1.457)	(1.368)	(-3.387)	(1.268)	(1.079)
δ_4	-0.083	-0.171**	0.015	-0.228	-0.087	0.342	-0.214	-0.117	0.363	-0.279	-0.092	0.332
	(-0.701)	(-2.392)	(0.068)	(-1.185)	(-0.56)	(1.28)	(-1.132)	(-0.648)	(1.352)	(-1.482)	(-0.332)	(1.292)
α	0.272***	0.119**	0.144***	0.222***	0.209***	0.194***	0.204***	0.146*	0.184***	0.184***	0.116***	0.183***
	(5.179)	(2.284)	(4.569)	(3.336)	(3.333)	(4.421)	(3.862)	(1.853)	(4.251)	(3.742)	(2.93)	(4.347)
β	0.463***	0.157	0.778***	0.655***	0.661***	0.716***	0.678***	0.753***	0.728***		0.824***	0.723***
	(5.388)	(0.819)	(18.946)	(5.896)	(6.812)	(13.936)	(8.042)	(4.819)	(14.406)	(8.511)	(14.072)	(14.32)
DCC Parameters												
λ_1	0.092*** (6.308)			0.131*** (5.607)			0.126*** (5.533)			0.126*** (5.013)		
λ_2	0.849*** (36.618)			0.805*** (22.705)			0.814*** (23.682)			0.802*** (19.401)		
$\rho_{\text{(banks, financials)}}$	0.751*** (13.808)			0.556*** (6.974)			0.548*** (6.483)			0.558*** (7.314)		
$\rho_{\text{(banks, insurance)}}$	0.580*** (7.850)			0.226** (2.124)			0.222** (2.017)			0.244** (2.468)		
$\rho_{\text{(insurance, financials)}}$	0.534*** (6.565)			0.149 (1.329)			0.126 (1.076)			0.120 (1.115)		
Model Fit												
Log Likelihood	-2,934.574			-2,716.250			-2,711.710			-2,679.870		
Panel B: Value-Weighted Portfolios												
Variance Equation												
δ_1	0.087	0.722*	0.066	0.124	-0.233	0.112	0.131	-0.198	0.124	0.13	-0.028	0.139
	(0.368)	(1.855)	(0.306)	(0.57)	(-0.368)	(0.494)	(0.609)	(-0.324)	(0.548)	(0.498)	(-0.043)	(0.608)
δ_2	-0.118	0.338	-0.316*	-0.349	0.277	-0.344*	-0.365*	0.284	-0.336*	-0.354	0.442	-0.344*
	(-0.514)	(0.915)	(-1.661)	(-1.686)	(0.631)	(-1.767)	(-1.79)	(0.65)	(-1.711)	(-1.48)	(0.87)	(-1.76)
δ_3	-0.292	0.358	0.441	-0.135	1.089*	0.407	-0.115	1.084**	0.402	-0.183	1.150**	0.472
	(-0.948)	(0.392)	(1.478)	(-0.488)	(2.335)	(1.403)	(-0.414)	(2.365)	(1.372)	(-0.503)	(2.147)	(1.643)
δ_4	0.097	-0.102	-0.205	-0.24	-0.762	-0.242	-0.251	-0.784	-0.254	-0.288	-0.757	-0.24
	(0.345)	(-0.134)	(-0.876)	(-1.101)	(-1.286)	(-0.945)	(-1.152)	(-1.35)	(-0.998)	(-1.135)	(-1.353)	(-0.924)
α	0.180***	0.167***	0.162***	0.177***	0.216***	0.175***	0.173***	0.214***	0.175***	0.177***	0.187***	0.181***
	(4.79)	(4.408)	(4.284)	(4.421)	(4.906)	(4.023)	(4.364)	(4.854)	(4.075)	(4.42)	(4.527)	(3.905)
β	0.731***	0.813***	0.752***	0.724***	0.795***	0.738***	0.728***	0.796***	0.738***	0.744***	0.822***	0.735***
	(14.537)	(21.231)	(15.237)	(12.844)	(22.655)	(12.616)	(12.932)	(22.535)	(12.828)	(14.542)	(25.511)	(12.177)
DCC Parameters												
λ_1	0.040*** (4.246)			0.053*** (3.391)			0.053*** (3.347)			0.040** (2.387)		
λ_2	0.933*** (66.173)			0.874*** (25.141)			0.878*** (24.673)			0.869*** (15.120)		
$\rho_{\text{(banks, financials)}}$	0.516*** (5.514)			0.400*** (5.677)			0.397*** (5.501)			0.350*** (5.593)		
$\rho_{\text{(banks, insurance)}}$	0.380*** (3.609)			0.282*** (3.587)			0.285*** (3.553)			0.308*** (4.583)		
$\rho_{\text{(insurance, financials)}}$	0.228** (1.965)			0.157* (1.900)			0.157* (1.852)			0.153** (2.211)		
Model Fit												
Log Likelihood	-3,123.495			-3,009.283			-3,008.171			-2,972.819		

Table 6: **Bank exposure and lending**

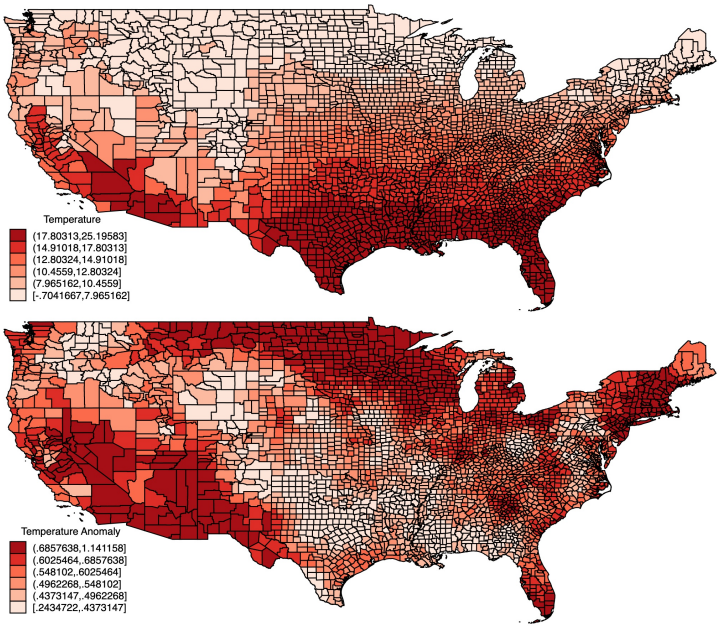
This table presents results linking credit outcomes at the county-bank-year level and the climate beta with respect to the first temperature anomaly factor. In columns (1)–(2), the dependent variable is the logarithm of the number of small farm loan originations by a bank to small businesses in a county-year. In columns (3)–(4), the dependent variable is the logarithm of the total loan amount extended by a bank to small businesses in a county-year. *Bank exposure* is the calendar year average of monthly climate betas estimated using time-series regression for each bank's stock returns on market and temperature anomaly factors. The independent variable is *lagged* by one year. The lagged control variables are the *capital ratio* that equals tier 1 capital as a fraction of total assets, *bank size* measured by the logarithm of the total assets of a bank, *profitability* that equals the return on assets, and *NPL-to-assets* that equals non-performing loans as a fraction of total assets of a bank. The sample period is from 1997 to 2017. The standard errors are clustered by county and bank, and *t*-statistics are in parentheses. Significance levels: * $p < 0.10$, ** $p < 0.05$, *** $p < 0.01$.

	(1)	(2)	(3)	(4)
	Dependent variable: Ln(·)			
	Number of originations		Loan volume	
Bank exposure	-0.3423**	-0.2016***	-0.2479**	-0.1118*
	(-2.1500)	(-3.2511)	(-1.9701)	(-1.8469)
Bank size		0.2739**		0.6107***
		(2.2193)		(6.2038)
Capital ratio		7.6838**		4.6720
		(2.1243)		(1.4137)
Profitability		9.7218**		6.3692*
		(2.1409)		(1.6660)
NPL-to-Assets		-5.1610		-8.1069
		(-0.3391)		(-0.6756)
N	457,788	457,752	457,788	457,752
R^2	0.8345	0.8429	0.8432	0.8481
County × Bank FE	✓	✓	✓	✓
County × Year FE	✓	✓	✓	✓

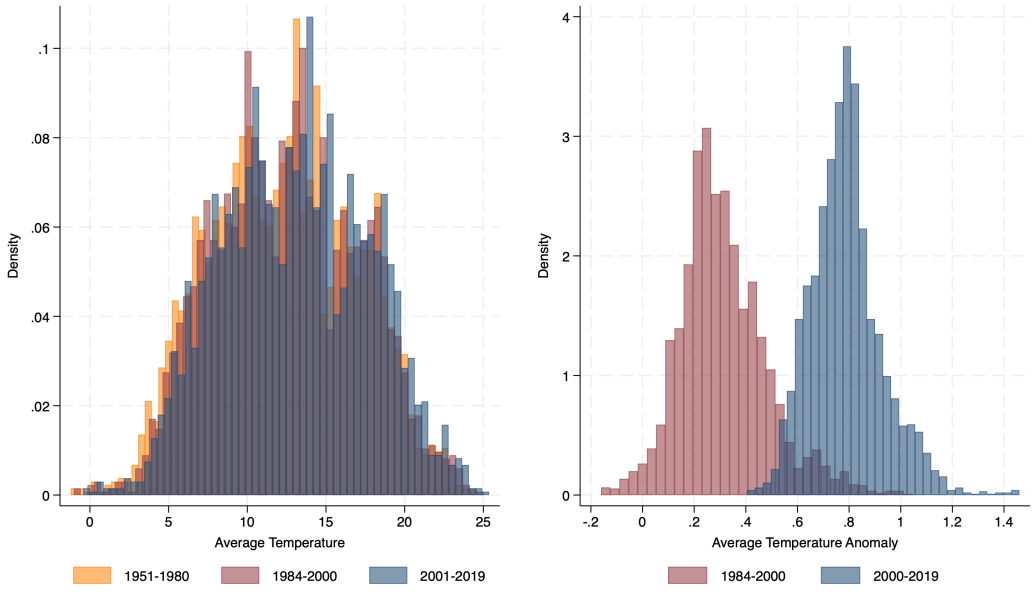
Table 7: **Bank exposure, branch network, and lending**

This table presents results linking credit outcomes at the county-bank-year level and the climate beta with respect to the first temperature anomaly factor for counties in and out of a bank's branch network. In columns (1)–(2), the dependent variable is the logarithm of the number of small farm loan originations by a bank to small businesses in a county-year. In columns (3)–(4), the dependent variable is the logarithm of the total loan amount extended by a bank to small businesses in a county-year. *Non-core market* is a dichotomous variable that equals 1 (0 otherwise) if a bank does not have a branch in a given county. *Bank exposure* is the calendar year average of monthly climate betas estimated using time-series regression for each bank's stock returns on market and temperature anomaly factors. The independent variable is *lagged* by one year. The lagged control variables are the *capital ratio* that equals tier 1 capital as a fraction of total assets, *bank size* measured by the logarithm of the total assets of a bank, *profitability* that equals the return on assets, and *NPL-to-assets* that equals non-performing loans as a fraction of total assets of a bank. The symbol # signifies that all controls and fixed effects are interacted with *non-core market* dummy variable to allow for heterogeneous effects across core and non-core markets. The sample period is from 1997 to 2017. The standard errors are clustered by county and bank, and *t*-statistics are in parentheses. Significance levels: * $p < 0.10$, ** $p < 0.05$, *** $p < 0.01$.

	(1)	(2)	(3)	(4)
	Dependent variable: Ln(·)			
	Number of originations		Loan volume	
Bank exposure×𝟙.Non-core market	-0.1837***	-0.1121*	-0.1393***	-0.0974
	(-3.1159)	(-1.7036)	(-2.6210)	(-1.5676)
Bank exposure	-0.0951	-0.1144**	-0.0382	-0.0436*
	(-1.5719)	(-2.2052)	(-0.6863)	(-1.7337)
𝟙.Non-core market	-1.1851***		-1.4675***	
	(-8.0165)		(-16.9725)	
N	457,752	457,752	457,752	457,752
R^2	0.8517	0.8853	0.8558	0.8801
Bank controls	✓	✓#	✓	✓#
County × Bank FE	✓	✓#	✓	✓#
County × Year FE	✓	✓#	✓	✓#



(a) Spatial distribution of monthly temperature and temperature anomaly



(b) Average temperature and temperature anomaly over different time periods

Figure 1: In Panel (a), the figure displays spatial maps of average temperature (top) and average temperature anomaly (bottom). Both are computed using data from 1984 to 2019. In Panel (b), the figure on the left shows the distribution of average temperatures across three non-overlapping periods: 1951–1980 (reference period), 1984–2000, and 2001–2019. The figure on the right in Panel (b) presents the distribution of temperature anomalies for 1984–2000 and 2001–2019, measured relative to the 1951–1980 baseline.

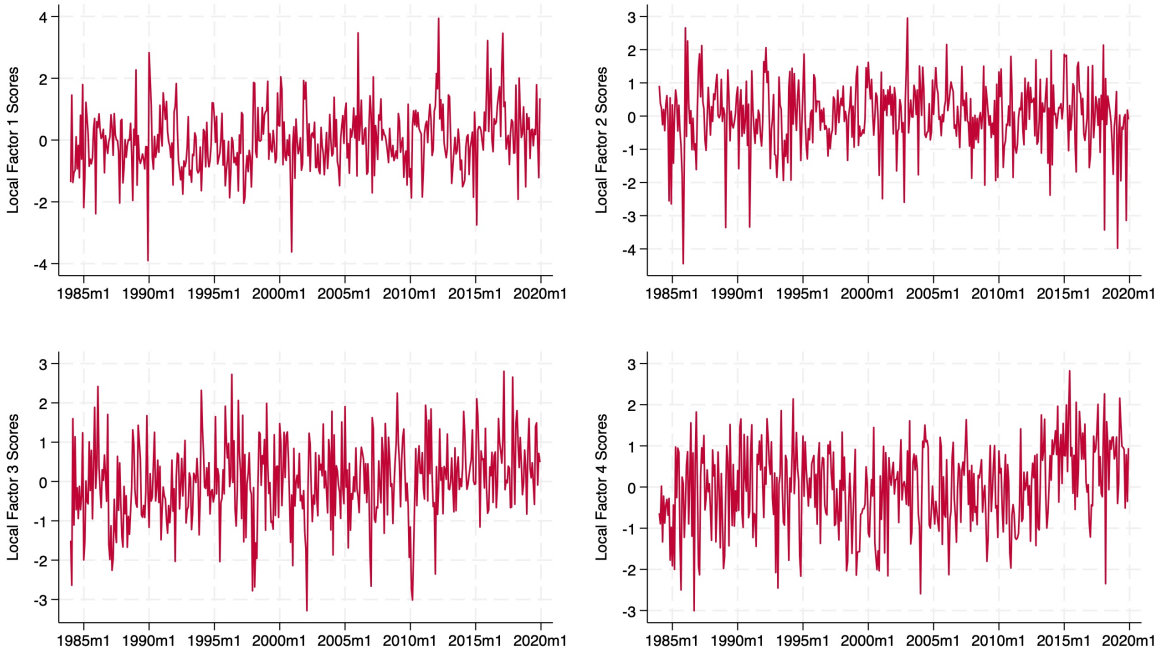
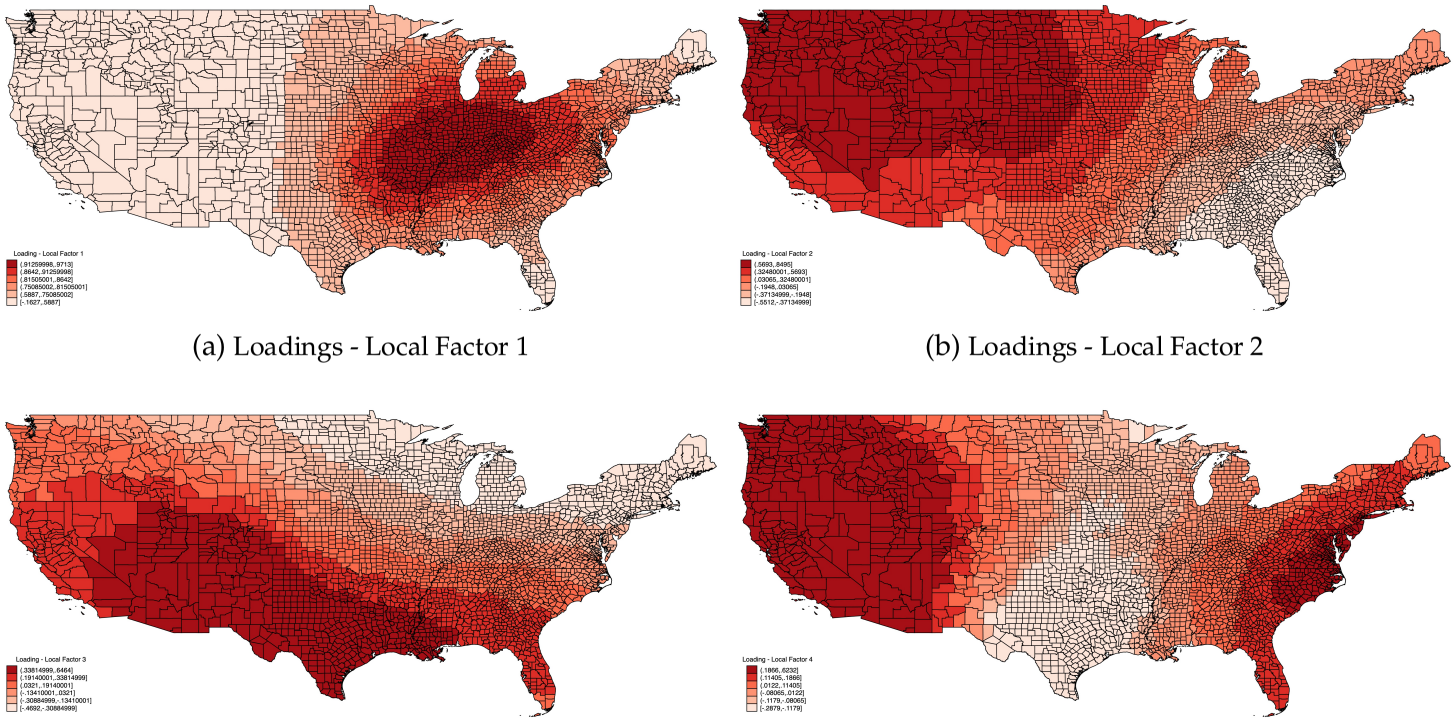


Figure 2: The figure shows the time series of temperature anomaly factor scores derived from factor analysis of temperature anomaly, covering the period from 1984 to 2019.



(a) Loadings - Local Factor 1

(b) Loadings - Local Factor 2

(c) Loadings - Local Factor 3

(d) Loadings - Local Factor 4

Figure 3: The figure shows the spatial distribution of counties' exposures to the first four temperature anomaly factors derived from factor analysis, based on monthly temperature anomaly data from 1984 to 2019 across US counties.

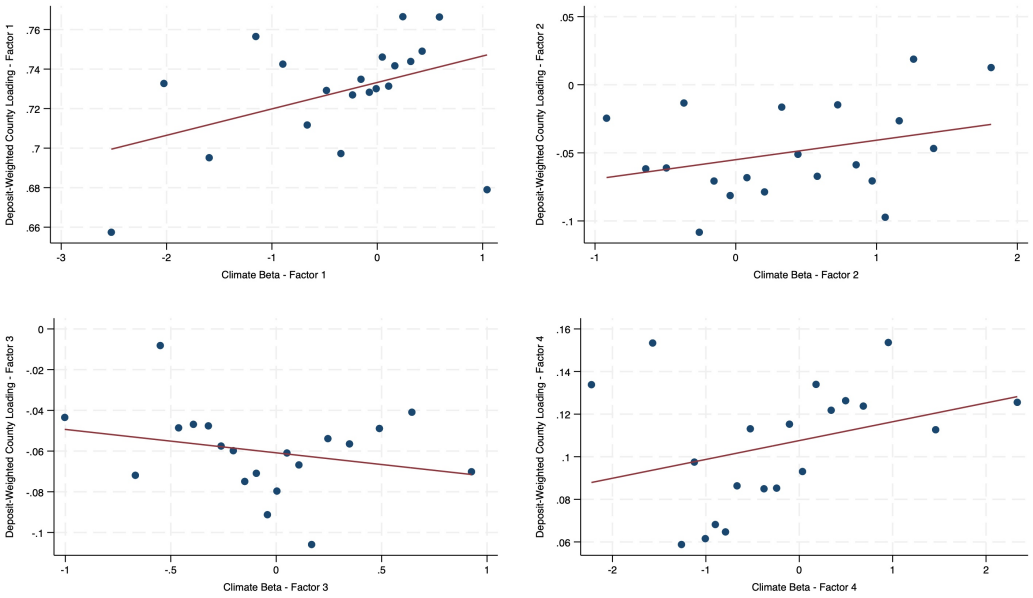


Figure 4: This figure presents binned scatter plots of deposit-weighted county loadings (y-axis) and banks' climate betas (x-axis). The deposit-weighted average loading for factor f is estimated as $\sum_c w_{cbt}\hat{\lambda}_{ck}$, where w_{cbt} equals $\frac{D_{cbt}}{D_{bt}}$ and D_{cbt} represents deposits of bank b across all branches in county c in year t. The sample period is from 1994–2019.

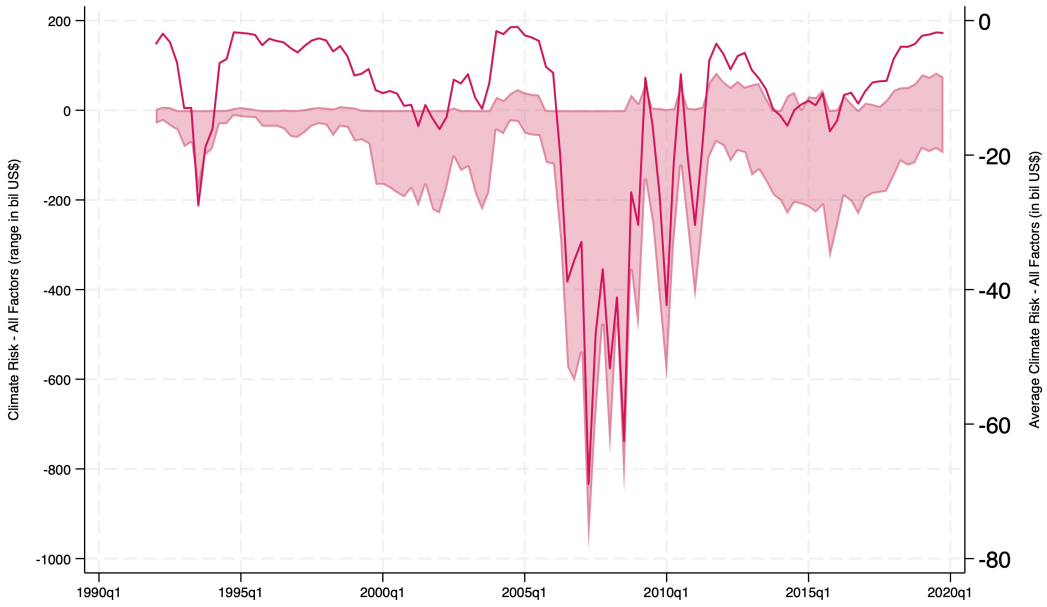
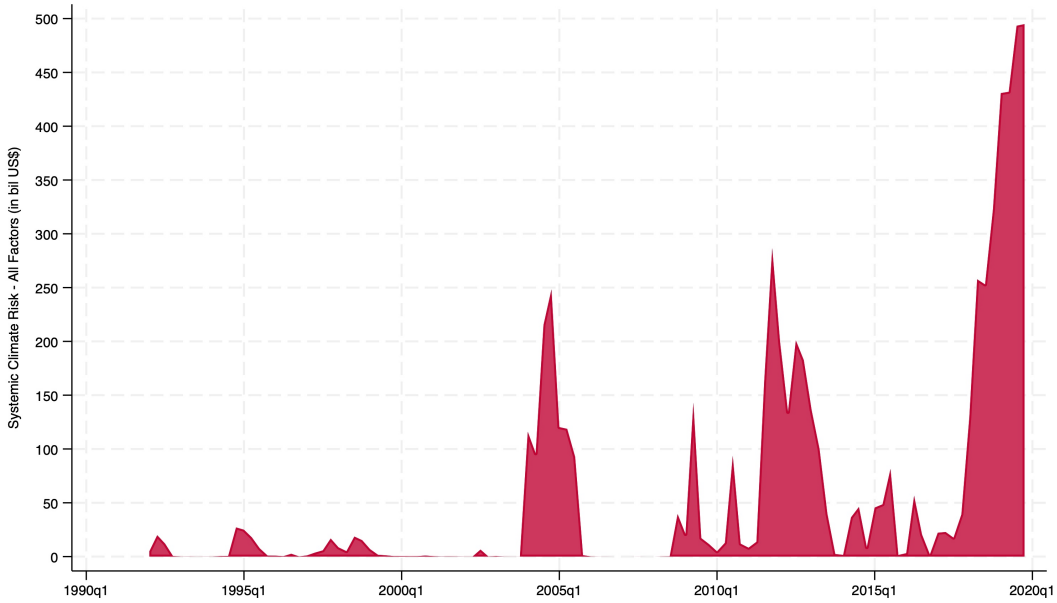
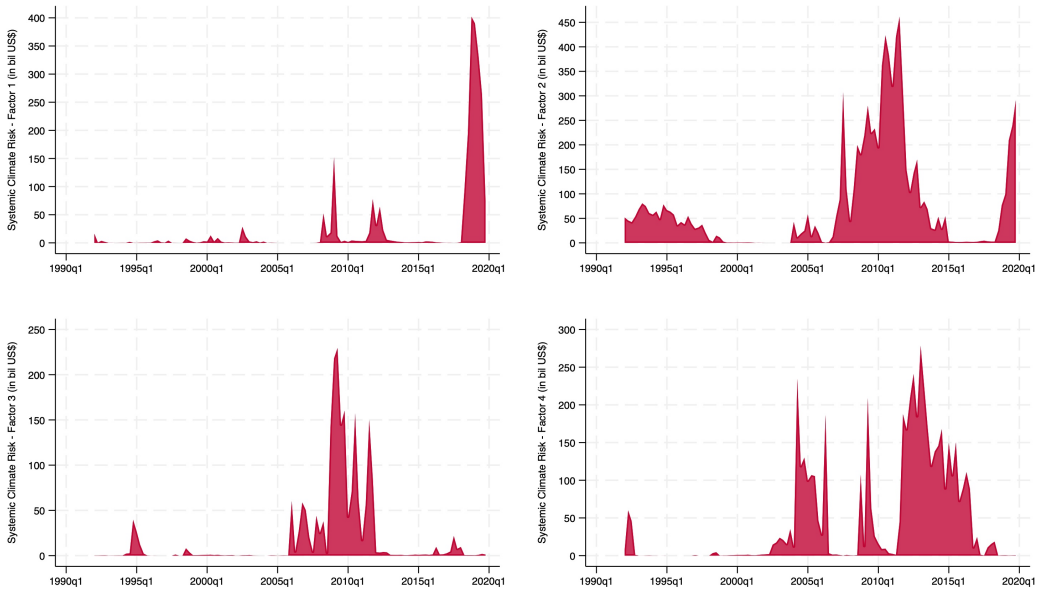


Figure 5: This figure illustrates the evolution of physical climate risk for US banks from 1992:Q1 to 2019:Q4. The solid line plots the cross-sectional average, while the shaded area captures the range between the most and least exposed institutions at each point in time. Positive values indicate insufficient capital to absorb physical climate shocks, reflecting heightened vulnerability. The figure summarizes the cumulative effect of all four temperature anomaly factors, providing a sector-wide view of physical climate risk and its dispersion across banks.



(a) Systemic Climate Risk



(b) Systemic Climate Risk–Disaggregated by Factor.

Figure 6: The figure presents the time series of systemic physical climate risk for publicly traded US banks from 1992:Q1 to 2019:Q4. Panel (a) shows the aggregate measure, combining the contributions of all four temperature anomaly factors. Panel (b) disaggregates this risk, displaying separate time series for each factor's contribution to systemic physical climate risk.

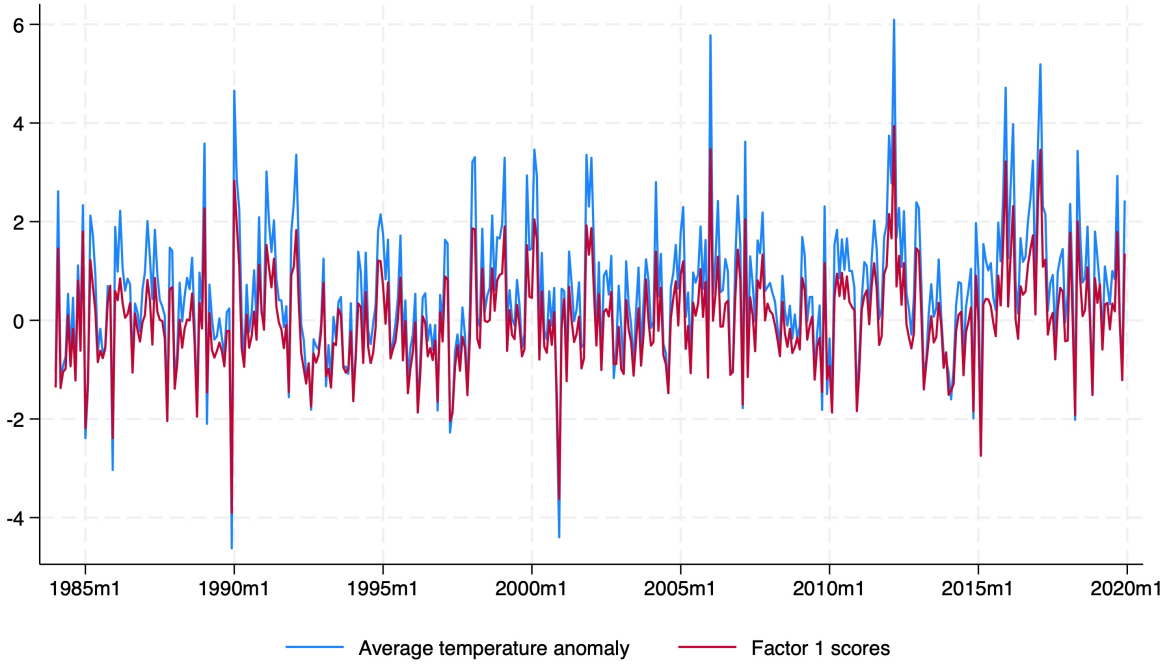


Figure 7: The figure shows the time series of scores for the first factor derived from factor analysis of global temperature anomaly and of the cross-sectional average of temperature anomaly across the contiguous US counties. The sample period spans from 1984 to 2019.

Online Appendix

How Exposed are Banks to Physical Climate Risk?

Appendix A: Addressing the rotational indeterminacy

This appendix operationalizes the geographic interpretation of the statistical factors. Because the unrotated factors align closely with geographic coordinates, we construct pre-specified "location-based" factors to verify that the statistical and geographic representations yield consistent results.

In Section 3.1, we utilize temperature anomaly factors estimated using factor analysis. While it reduces dimensionality, this approach is purely statistical in nature, which limits the direct economic interpretation of the factors. Factor rotation can enhance interpretability but introduces subjectivity and alters numerical representations without affecting explanatory power. Retaining unrotated factors preserves the statistical structure, ensuring consistency and comparability.

To improve interpretability, we construct pre-specified physical risk factors. Figure 3 shows that county loadings exhibit geographic patterns along latitude and longitude. For example, Factor 1 loads more positively on the US East Coast than on the West, while Factor 4 loads positively on both coasts, suggesting that ocean proximity influences its loadings. We standardize geographic coordinates for all contiguous US counties by differencing out the latitude and longitude of Lebanon, Kentucky (latitude 38.8282, longitude 98.5796). Next, we estimate the following cross-sectional regression each month:

$$\begin{aligned}\Delta\mathbb{T}_{ct} =& \alpha + \beta_{1t}\text{Latitude}_c + \beta_{2t}\text{Longitude}_c + \beta_{3t}\text{Latitude}_c \times \text{Longitude}_c + \\ & \beta_{4t}\text{Latitude Squared}_c + \beta_{5t}\text{Longitude Squared}_c + u_{ct} \qquad \forall \quad t\end{aligned} \tag{A.1}$$

In equation (A.1), $\Delta\mathbb{T}_c$ represents the temperature anomaly for county c. The squared latitude term captures the non-linear relationship between latitude and temperature anomalies, as regions farther from the equator experience greater deviations from historical norms. The squared longitude term reflects proximity to oceans. The set of β coefficients provides a time series of five geographic factors–latitude, longitude, latitude×longitude, latitude squared, and longitude squared–where county loadings correspond to their respective standardized geographic coordinates.

	N	Mean	SD	Min	Max	CoV
Latitude Factor	432	0.014	0.113	-0.399	0.395	8.123
Longitude Factor	432	-0.002	0.046	-0.146	0.181	23.449
Latitude×Longitude Factor	432	0.000	0.003	-0.009	0.008	15.410
Latitude Squared Factor	432	0.001	0.009	-0.041	0.030	8.222
Longitude Squared Factor	432	0.000	0.002	-0.006	0.006	31.602

Table A.1: This table presents the summary statistics of location-based factors. The statistic CoV is the coefficient of variation estimated as the absolute value of the standard deviation scaled by the mean.

Table A.1 reports summary statistics, and Figure A.1 plots the time series of five location-based factors. The (latitude-) longitude-based factors display greater (lower) variability as their coefficients of variation are (low) high. These patterns suggest short-run swings in longitude-based factors drive much of the volatility in east–west climate patterns, which may be especially relevant for sectors sensitive to such shifts.

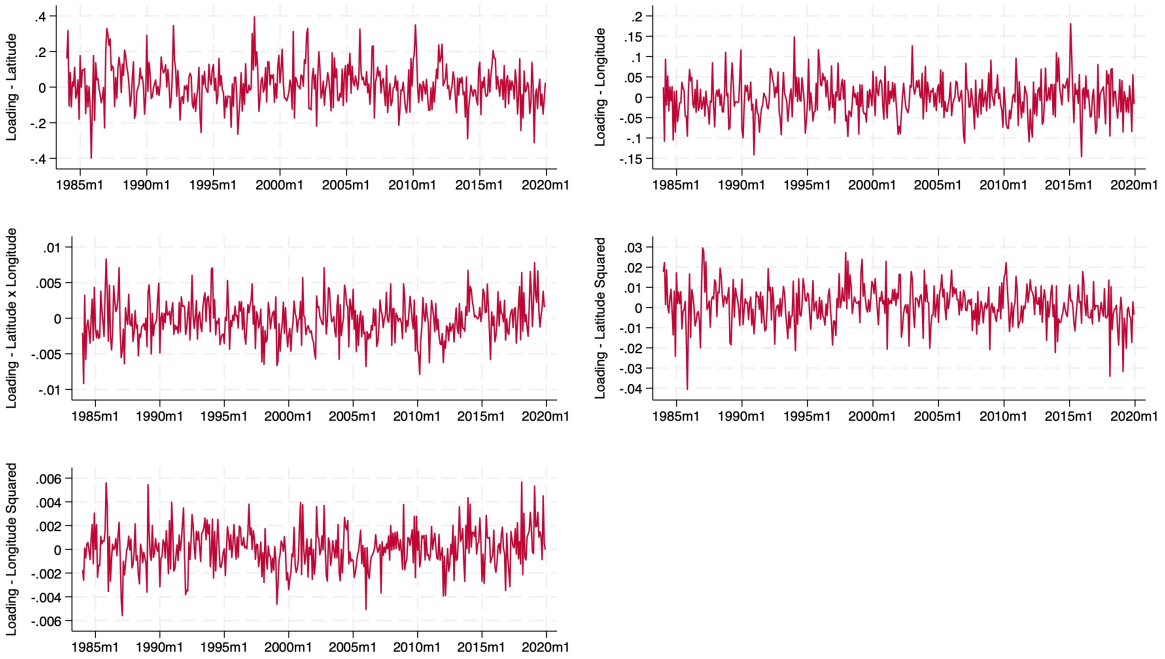


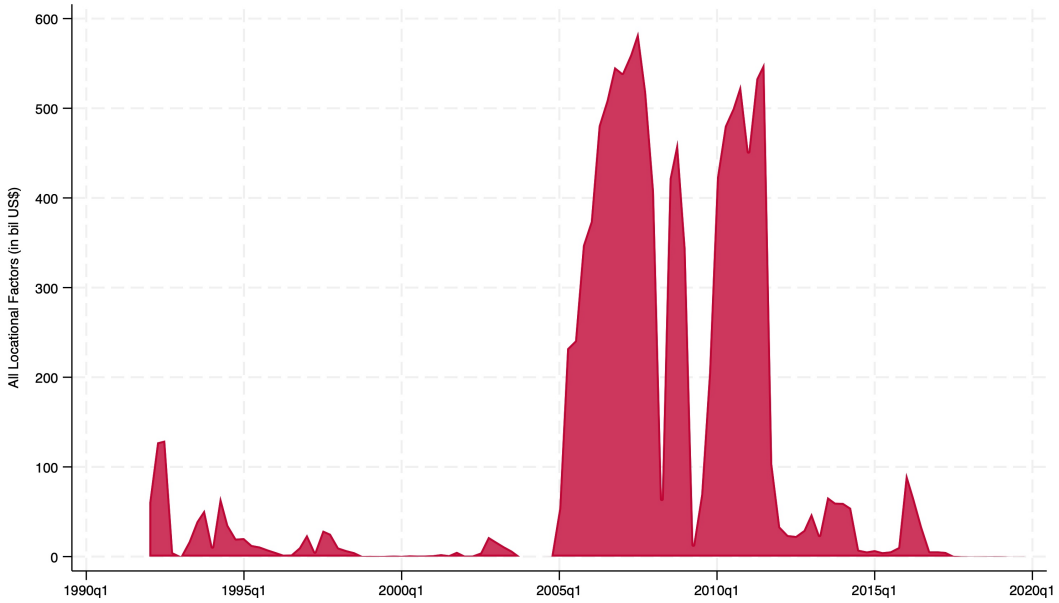
Figure A.1: The figure shows the time series of location-based factor scores, covering the period from 1984 to 2019.

In Table A.2, we present correlations between the statistical factors extracted via factor analysis and those extracted using Fama-MacBeth regressions by pre-specifying county loadings based on de-meaned geographic coordinates. The bottom row summarizes the highest absolute correlation for each statistical factor across the five location-based factors. These magnitudes indicate that systematic variation in temperature anomalies across US counties aligns closely with predictable geographic patterns.

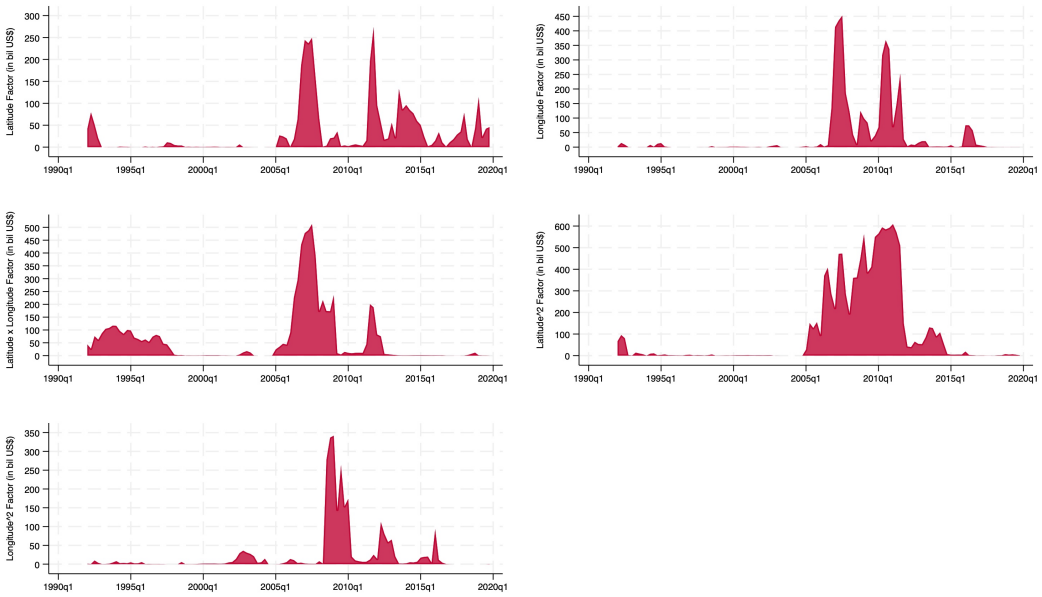
	Local Factor 1	Local Factor 2	Local Factor 3	Local Factor 4	Highest |value|
Latitude Factor	0.368	0.529	-0.744	-0.058	0.744
Longitude Factor	-0.571	0.582	0.565	0.074	0.582
Latitude×Longitude Factor	-0.226	-0.516	0.548	0.309	0.548
Latitude Squared Factor	0.022	0.725	-0.479	-0.362	0.725
Longitude Squared Factor	-0.389	-0.785	0.049	0.377	0.785
Highest |value|	0.571	0.785	0.744	0.377	

Table A.2: This table presents correlations between location-based factors and local temperature anomaly factors extracted via factor analysis in Section 3.1.

Using these location-based factors, we estimate the systemic physical climate risk and present its time series in Figure A.2. Unlike the baseline results using temperature anomaly factors, these estimates peak between 2005 and 2014 (Figure A.2a), with considerable variation across individual factors (Figure A.2b). This temporal divergence reflects the structural differences between statistical factors and pre-specified geographic factors. Location-based factors incorporate two channels: vulnerability to climate shocks and adaptive capacity shaped by geography. While climate change drives both disaster frequency and adaptation responses, location-based factors likely reflect their net effect. Temperature anomaly factors estimated via factor analysis offer a parsimonious way to estimate physical climate risk, abstracting from spatial location per se and focusing on common patterns of temperature fluctuation.



(a) Systemic climate risk estimated using location-based factors



(b) Systemic climate risk–Disaggregated by location-based factor.

Figure A.2: The figure presents the time series of systemic physical climate risk for publicly traded US banks from 1992:Q1 to 2019:Q4, estimated using location-based factors. Panel (a) displays the aggregate measure, which combines the contributions of all location-based factors. Panel (b) disaggregates this risk, displaying separate time series for each factor's contribution to systemic physical climate risk.

Appendix B: Estimating physical climate risk using global temperature data

We construct a dataset with global gridded temperature anomalies mapped onto 1,785 sub-national administrative units (states). We apply factor analysis to extract latent temperature anomaly factors from this dataset using the approach outlined in Section 3.1. As shown in Panel of Table B.1, the first four factors explain 46 percent of temperature anomaly variation across 1,785 regions over 36 years (beginning in January 1984). The first four factors explain 20.0, 13.2, 7.8, and 4.5 percent of the variation in temperature anomalies across 1,785 global regions, respectively.

Panel A: Global factor analysis output

	Eigenvalue	Difference	Proportion	Cumulative
Global - Factor 1	355.457	119.926	0.199	0.199
Global - Factor 2	235.532	97.257	0.132	0.331
Global - Factor 3	138.275	57.749	0.078	0.409
Global - Factor 4	80.527	11.220	0.045	0.454

Panel B: Correlation between local and global temperature anomaly factors

	Local - Factor 1	Local - Factor 2	Local - Factor 3	Local - Factor 4
Global - Factor 1	0.164	0.083	0.045	0.196
Global - Factor 2	0.088	-0.060	-0.021	0.165
Global - Factor 3	-0.272	0.110	0.218	-0.049
Global - Factor 4	0.338	-0.132	0.042	-0.068

Table B.1: This table presents the output of *global* factor analysis implemented on the sub-national-month-year level temperature anomaly. Here, temperature anomaly, denoted $\Delta\mathbb{T}_{smy} = \mathbb{T}_{smy} - \frac{1}{30}\sum_{y=1951}^{1980}\mathbb{T}_{smy}$. The subscripts s, m, and y represent sub-national region, month, and year, respectively. In Panel A, we present the eigenvalues of the first four factors and the proportion of the total variation in monthly temperature anomaly across the globe. In Panel B, we present correlations between the first four local temperature anomaly factors estimated using US county-level temperature anomaly data and global temperature anomaly factors. The sample period spans 36 years (1984:M1–2019:M12).

Panel B of Table B.1 reports the correlations between the first four global temperature anomaly factors and their counterparts estimated using US county-level data. The correlations between global and local factors are low, implying that local and global temperature anomaly factors are not simple proxies for each other and that local temperature anomalies exhibit spatial heterogeneity not fully explained by global average temperature. This distinction underscores the need to evaluate the relevance of global factors empirically, rather than assuming they amplify or substitute for local effects.

Figure B.1 shows the time series and Figure B.2 plots the loadings of the global temperature anomaly factors. The first factor is consistent with the global warming trend. The loadings first factor are higher for tropical regions such as Central Africa, South America, and Southeast Asia. For the second factor loadings concentrated in higher latitudes, including Europe, Russia, and parts of the Americas, regions that appear more sensitive to short-term swings in global temperature. The third factor follows a cyclical pattern, with marked peaks in the late 1990s and early 2010s. Loadings are positive in the Middle East, Central Asia, and Eastern Europe, and negative in parts of the Americas and Africa, highlighting regional divergence in medium-term climate patterns. The fourth factor also displays cyclical dynamics, with positive loadings in the

US Midwest and East Coast, Eastern Europe, and Southeast Asia, and negative loadings across much of Africa, South America, and Oceania.

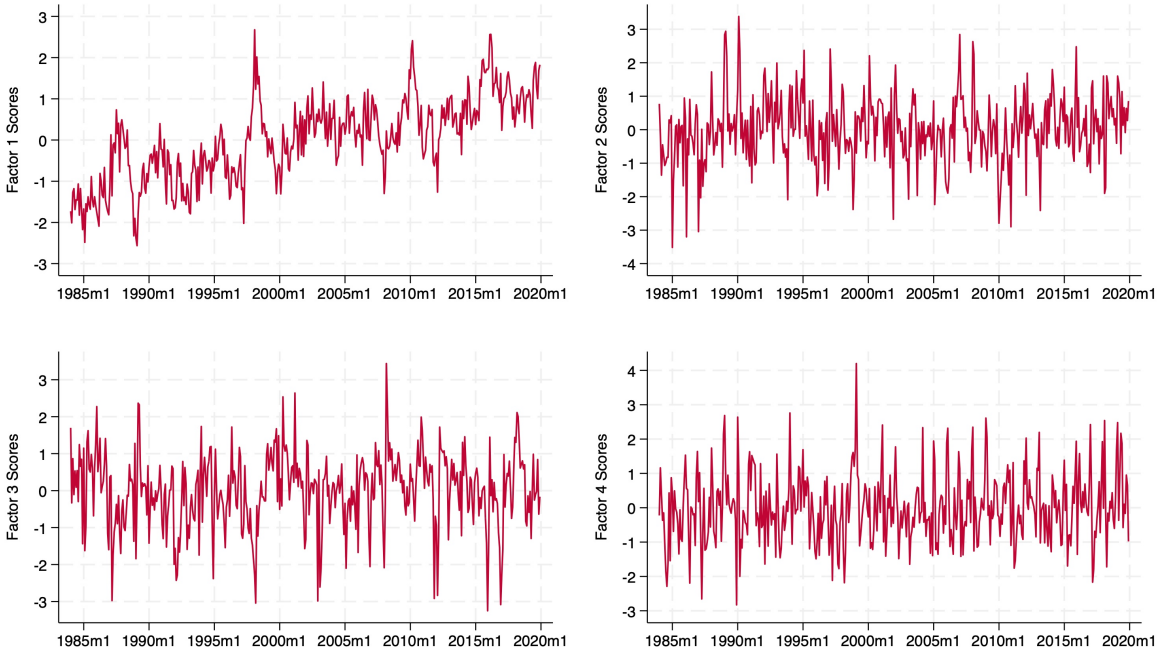
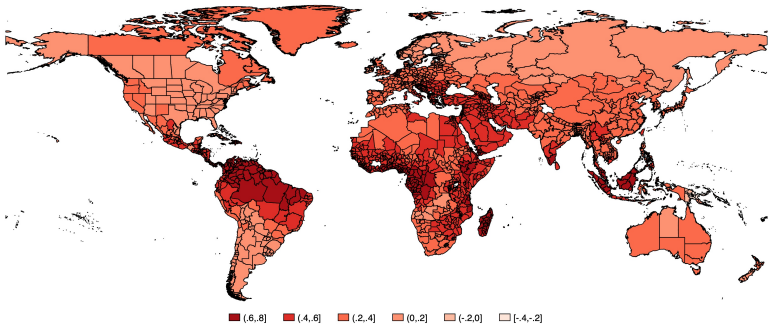
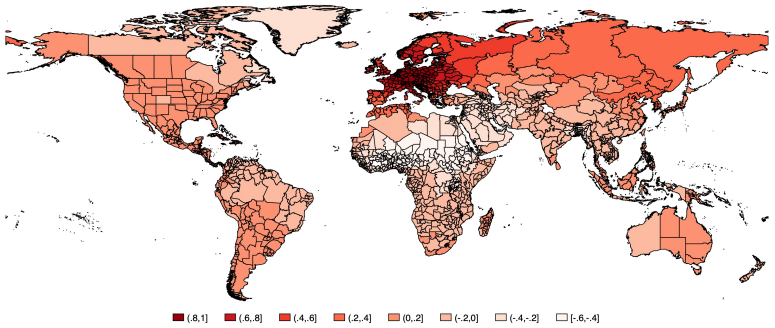


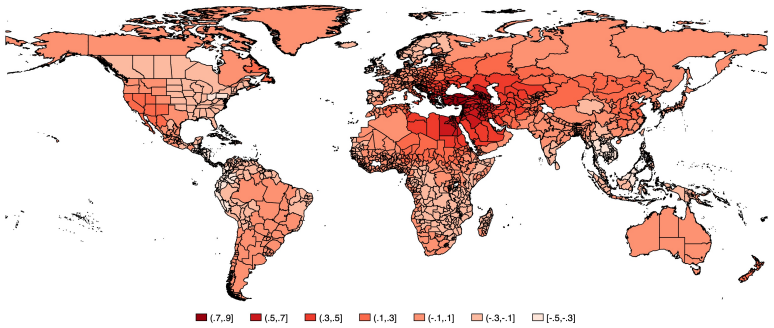
Figure B.1: The figure shows the time series of factor scores derived from factor analysis of global temperature anomaly, covering the period from 1984 to 2019.



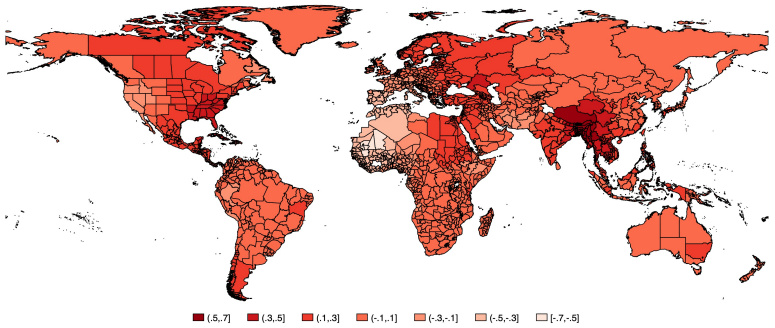
(a) Loadings - Global Factor 1



(b) Loadings - Global Factor 2



(c) Loadings - Global Factor 3



(d) Loadings - Global Factor 4

Figure B.2: The figure shows the spatial distribution of global regions' exposures to the first four temperature anomaly factors derived from factor analysis, based on monthly temperature anomaly data from 1984 to 2019 globally.

Using global temperature anomaly factors, we estimate systemic physical climate risk for the US banking sector. Figure B.3 presents the time series of systemic climate risk derived from these global factors. The estimated risk peaks at approximately 470 billion dollars. The largest peaks coincide with the Global Financial Crisis of 2008–2009 and the European sovereign debt crisis of 2012–2013. Banks' exposures are concentrated in specific regions through the geographic distribution of loans, collateral, and counterparties. These results suggest that during periods of financial distress, when banks are already vulnerable, global climate variation can add to the strain.

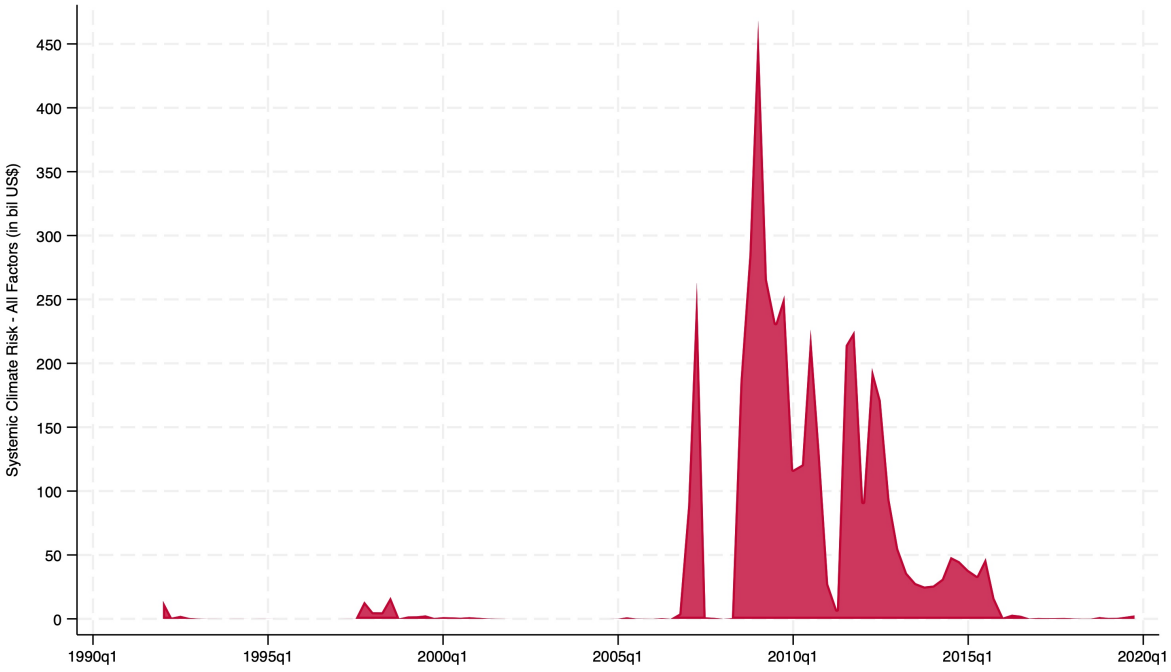


Figure B.3: The figure displays the time series of systemic physical climate risk for publicly traded US banks due to global temperature anomaly factors from 1992:Q1 to 2019:Q4.

Appendix C



Figure C.1: This figure plots the proportion of total cross-location variation in monthly temperature anomalies explained by the first four common factors. For each end year $Y \in \{2001, 2002, \cdots, 2019\}$, factors are estimated using an expanding monthly sample that begins in January 1984 and ends in December Y. The vertical axis reports the share of total variance explained by each factor, while the horizontal axis indexes the ending year of the expanding estimation window.

Table C.1: **Summary Statistics**

This table presents the summary statistics of key variables used in Tables 6 and 7 in the main text. The number of originations and loan volume corresponds to the total number and volume of small business loans originated by a bank in a county-year. These data are reported to the Federal Financial Institutions Examinations Council (FFIEC) under the Community Reinvestment Act. Bank size equals the logarithm of total assets. Capital ratio is defined as the ratio of equity to total assets. Profitability is defined as operating income as a percentage of total assets. NPL-to-Assets is the ratio of loan loss provisions as a fraction of total assets. The sample period spans 21 years, starting in 2017 and ending in 2017.

	N	Mean	SD	p10	p25	p50	p75	p95
Ln(Number of originations)	457,752	2.2022	1.6681	0.0000	0.6931	1.9459	3.3673	4.5850
Ln(Loan volume)	457,752	5.8862	2.1805	3.0445	4.3175	5.9054	7.4128	8.7760
Exposure - Factor 1	457,752	-0.4484	0.8433	-1.9007	-0.8484	-0.1393	0.1253	0.3056
Bank Size	457,752	17.8471	2.2345	14.6794	16.2215	18.2109	19.3888	21.0281
Capital Ratio	457,752	0.1123	0.0440	0.0752	0.0877	0.1023	0.1226	0.1535
Profitability	457,752	0.0184	0.0293	0.0109	0.0121	0.0156	0.0207	0.0300
NPL-to-Assets	457,752	0.0022	0.0041	0.0001	0.0004	0.0008	0.0022	0.0064

Table C.2: **Summary statistics of bank climate betas**

This table reports summary statistics for banks' estimated temperature-anomaly betas (climate betas) with respect to the first four systematic temperature-anomaly factors. The quarterly climate betas are average betas over calendar months. The statistics are computed from a panel of 4,081 banks observed over an average of 21.8 quarters between 1992:Q1 and 2019:Q4.

Climate Beta	N	n	T	Mean	Standard Deviation		
					Overall	Between	Within
Factor 1	88,909	4,081	21.786	-0.396	0.834	0.540	0.748
Factor 2	88,909	4,081	21.786	0.525	0.757	0.550	0.626
Factor 3	88,909	4,081	21.786	-0.178	0.581	0.463	0.495
Factor 4	88,909	4,081	21.786	-0.293	0.940	0.583	0.831

Table C.3: **Bank Characteristics and Climate Betas**

This table reports regression results examining the association between bank characteristics and climate betas. The dependent variables are climate beta with respect to the first four temperature anomaly factors. We consider three bank characteristics: bank size (the logarithm of bank assets), capital ratio (equity to total assets ratio), and deposit entropy, a funding diversification measure. The entropy-based measure is calculated as $\sum_c S_{cbt} \log\left(\frac{1}{S_{cbt}}\right)$, where S_{cbt} denotes the deposit share of county c in bank b's total deposits in year t. The climate betas correspond to the average monthly beta across April, May, and June, and the call reports data correspond to the second quarter of the year. This temporal mapping aligns with the annual frequency of the summary of deposits data, which corresponds to the end of the second quarter (June). These choices ensure a yearly panel with consistent timing across all data sources. The sample covers 1994 to 2019. Standard errors are clustered by bank, with t-statistics in parentheses. Significance: * $p < 0.10$, ** $p < 0.05$, *** $p < 0.01$.

	(1)	(2)	(3)	(8)
	Dependent variable: Climate beta			
	Factor 1	Factor 2	Factor 3	Factor 4
Bank size	-0.035**	-0.001	0.023*	0.005
	(-2.097)	(-0.073)	(1.780)	(0.217)
Capital ratio	-0.282	0.598**	0.070	-0.098
	(-1.140)	(2.262)	(0.333)	(-0.286)
Deposit entropy	0.033**	0.014	-0.039***	0.001
	(2.122)	(0.732)	(-2.981)	(0.063)
N	15,553	15,553	15,553	15,553
R^2	0.917	0.801	0.736	0.887
Bank FE	✓	✓	✓	✓
Year FE	✓	✓	✓	✓

Table C.4: **Bank exposure and lending – Robustness**

This table presents results linking credit outcomes at the county-bank-year level and the climate beta with respect to the first temperature anomaly factor for counties in and out of a bank's branch network. In columns (1) and (3), the dependent variable is the logarithm of the number of small farm loan originations by a bank to small businesses in a county-year. In columns (2) and (4), the dependent variable is the logarithm of the total loan amount extended by a bank to small businesses in a county-year. *Non-core market* is a dichotomous variable that equals 1 (0 otherwise) if a bank does not have a branch in a given county. *Bank exposure* is the calendar year average of monthly climate betas estimated using time-series regression for each bank's stock returns on market and temperature anomaly factors. The independent variable is *lagged* by one year. The lagged control variables are the *capital ratio* that equals tier 1 capital as a fraction of total assets, *bank size* measured by the logarithm of the total assets of a bank, *profitability* that equals the return on assets, *NPL-to-assets* that equals non-performing loans as a fraction of total assets of a bank, and *realized volatility* that equals squared excess returns. The symbol # signifies that all controls and fixed effects are interacted with *non-core market* dummy variable to allow for heterogeneous effects across core and non-core markets. The sample period is from 1997 to 2017. The standard errors are clustered by county and bank, and *t*-statistics are in parentheses. Significance levels: * $p < 0.10$, ** $p < 0.05$, *** $p < 0.01$.

	(1)	(2)	(3)	(4)
	Dependent variable: Ln(·)			
	Number of originations	Loan volume	Number of originations	Loan volume
Bank exposure	-0.2011***	-0.1117*	-0.1139**	-0.0447*
	(-3.1815)	(-1.8460)	(-2.1892)	(-1.8051)
Bank exposure×𝟙.Non-core market			-0.1129*	-0.0962
			(-1.6889)	(-1.5504)
N	457,752	457,752	457,752	457,752
R^2	0.8429	0.8481	0.8853	0.8801
Bank controls	✓	✓	✓#	✓#
County × Bank FE	✓	✓	✓#	✓#
County × Year FE	✓	✓	✓#	✓#